AD NUMBER

AD417559

LIMITATION CHANGES

TO:

Approved for public release; distribution is unlimited. Document partially illegible.

FROM:

**Distribution authorized to U.S. Gov't. agencies and their contractors;
Administrative/Operational Use; APR 1963. Other requests shall be referred to Defense Advanced Research Projects Agency, ASBD-TIO, 675 North Randolph Street, Arlington, VA 22203-2114. Document partially illegible.**

AUTHORITY

mit/ll ltr via darpa, 2 may 1966

DISCLAIMER NOTICE

THIS DOCUMENT IS THE BEST QUALITY AVAILABLE.

COPY FURNISHED CONTAINED A SIGNIFICANT NUMBER OF PAGES WHICH DO NOT REPRODUCE LEGIBLY.

Improvement of the Measurement Capability of the FPQ Radar at Wallops Island

No. 505

Lincoln Laboratory

MASSACHUSETTS INSTITUTE OF TECHNOLOGY

LINCOLN LABORATORY

IMPROVEMENT OF THE MEASUREMENT CAPABILITY OF THE UHF RADAR AT WALLOPS ISLAND

J. FREEDMAN, Editor

Division 4

TECHNICAL REPORT NO. 305

10 APRIL 1963

ABSTRACT

A modification program was undertaken to improve the range resolution of the UHF radar at Wallops Island from 1000 to 200 ft, and to extend the ability to measure unambiguous Doppler velocity from 400 to 1200 ft/sec. This program was successfully completed in December of 1962. The ability to measure details of wake characteristics has been improved by these modifications beyond that possible with other radar re-entry measurement systems now in operation. Data taken by this radar should prove of interest in extending our knowledge of the characteristics of re-entry trails.

LEXINGTON MASSACHUSETTS

LIST OF CONTRIBUTORS

Andrews, W. A.	Group 46
Blake, C.	Group 46
Bromaghim, D. R.	Group 41
Butman, R. C.	Group 48
Drury, W. H.	Group 41
Freedman, J.	Division 4
Galvin, A. A.	Group 41
Jores, C. W.	Group 46
Mayer, D. F.	Group 47
Perry, J. P., Jr.	Group 47
Silverman, E.	Group 48
Spoerri, S.	Group 41

In addition to the individuals listed above as specific contributors to this report, we wish to acknowledge Aaron Galvin's assistance in preparing the report and the important contributions of David A. Cahlander and Eino O. Gronroos to subsystems tests and system integration. Other members of the Laboratory, too numerous to mention, from Division 3 and 4 and the Wallops Island Station also contributed time and effort to this project.

TABLE OF CONTENTS

IMPROVEMENT OF THE MEASUREMENT CAPABILITY OF THE UHF RADAR AT WALLOPS ISLAND

I. INTRODUCTION

A. Radar Backscatter from Re-entry Wakes

When a re-entry vehicle (RV) enters the earth's atmosphere, exchanges of energy take place between the vehicle and the atmosphere. Among the many consequences, an ionized trail is generated in the wake of the body. Recent experiments in hypervelocity tunnels indicate that, at some distance behind the re-entry body, the trail becomes turbulent. At a distance approximately 100 body diameters behind the re-entry body, it is believed that the mean velocity of the trail will decrease to perhaps less than 10 percent of the re-entry body's velocity and that the dispersion in velocity due to turbulence will be of the same magnitude.

The backscatter from the trail as observed by a radar with very good range and velocity resolution might have an amplitude and velocity characteristic as shown in Fig. 1(a-b). A possible variation of amplitude as a function of distance (x) behind the RV is shown in Fig. 1(a). A possible variation of velocity as a function of distance behind the RV is shown in Fig. 1(b). The shaded region indicates the range of fluctuation due to the turbulence.

In Fig. 2(a-b) an attempt is made to indicate the sort of velocity spectral distributions which may be observed at the head of the trail and at some point farther along the trail. The length of the trail may be on the order of several thousands of feet. The velocity of the RV (v_o) may be on the order of 20,000 feet per second (ft/sec). In order to obtain moderately well-resolved measurements of range and velocity, range resolution on the order of 100 ft and velocity resolution on the order of 1000 ft/sec are necessary. To date, no available radar has provided simultaneously such resolution in range and velocity.

The Radar Division (Division 4) of Lincoln Laboratory is modifying the TRADEX radar to provide this order of resolution. These modifications will not be completed and in operation until the summer of 1963. The AMRAD radar, based on signal designs provided by Division 4, will also have this resolution. It will not be operational until the winter of 1963.

If an observation is made by a radar incapable of resolving in range but with moderate Doppler resolution, then a velocity distribution such as illustrated in Fig. 3 may be observed. Several observations of this sort have been made. The Millstone Hill UHF radar, which has a pulse length of 2000 μsec (and hence a range resolution of 166 n.mi and a Doppler resolution of 500 cps), has been used to observe a Wallops Island firing. A result similar to that shown in Fig. 3, but somewhat coarser, was obtained because of the limited Doppler resolution. Therefore, it was possible to determine only that the turbulent velocity in the wake was less than or equal to 500 cps. Similar observations have been made on other RVs by the Trinidad radar, which has characteristics identical to the Millstone Hill radar. Similar results were obtained on both radars.

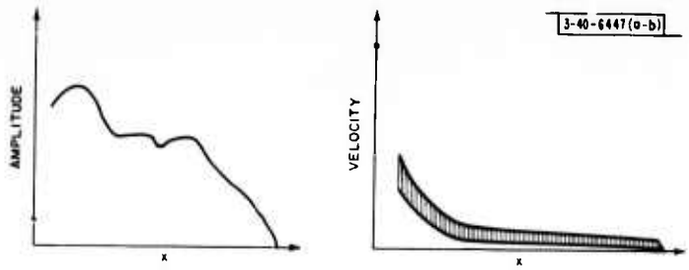

(a) Amplitude characteristic. (b) Velocity characteristic.

Fig. 1. Possible variation of amplitude and velocity of turbulent wake as a function of distance behind the RV.

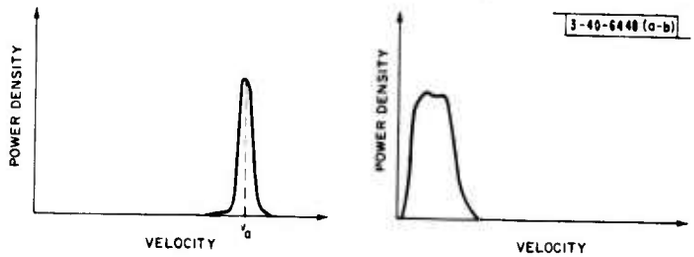

(a) Range segment including the RV.

(b) Range segment near far end of wake.

Fig. 2. Possible velocity distributions in a turbulent wake.

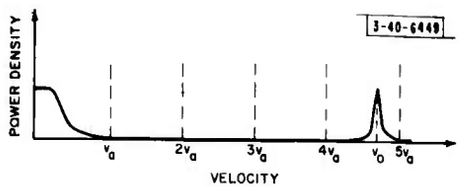

Fig. 3. Possible velocity distribution which might be observed by a radar system incapable of resolving the turbulent wake in range, but having velocity resolution and no velocity ombiguity.

If an observation is made by a radar with adequate Doppler resolution but with Doppler ambiguities, the results will differ from those shown in Fig. 3. The ambiguities are related to the sampling rate of the radar (i.e., its prf) and a fold-over of the spectrum occurs. Two cases are shown in Fig. 4(a-b). In Fig. 4(a), the result of a sampling rate is shown which folds over the data at velocity intervals v_a indicated by the dotted lines in Fig. 3. A sampling rate on the order of 1000 pulses per second (pps) is required to obtain this sort of result. Information concerning the trail turbulence can be obtained in spite of the ambiguities. The peak due to the RV will not remain stationary. Spectra taken at different times will show this peak at different velocities. The spectral region due to turbulence does remain in the neighborhood of zero velocity. If moderate range resolution is introduced, then separate spectra somewhat similar to that of Fig. 2 will be obtained.

If a sampling rate is used which is lower than the spectral distribution of the trail, then a folded spectrum will be obtained, as shown in Fig. 4(b). No deductions concerning trail turbulence other than that it is greater than the sampling frequency can be made from such data.

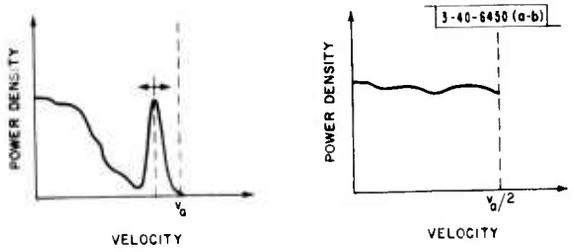

(a) Sampling rate = $2v_a/\lambda$. (b) Sompling rate $\leq v_a/\lambda$.

Fig. 4. Possible velocity distributian abservable by a radar system having good velocity resalution, but with velacity ambiguity, and incapable af resalving the turbulent wake in ronge.

In the early phase of operation at Wallops Island, the radars were able to measure amplitude only, and with a resolution of several thousand feet. Only approximate estimates of trail length could be made, and no real development of the amplitude variation as a function of distance behind the RV could be determined.

Division 4 modified the UHF radar to permit measurement of the radial velocity, but with ambiguities due to the pulse repetition rate. The ambiguous velocity due to a repetition rate of 300 cps is approximately 400 ft/sec at this radar frequency. Velocity spectra were obtained which proved to be similar to the one in Fig. 4(b). The sampling rate was too low and the pulse width too large. It was therefore possible to confirm only that the trail was turbulent with a turbulence dispersion greater than 300 cps.

Calculations based on hypervelocity experiments plus data taken with the Millstone and Trinidad radars indicate that the extent of the velocity spectrum due to turbulence corresponded to about a 500-cps Doppler spectrum at UHF. Therefore, an increase of prf of about a factor of three would be adequate to permit spectra of the sort sketched in Fig. 4(a).

The pulse width of the UHF radar had been reduced from 6 to 1 μsec, giving a range resolution of about 1000 ft. This did provide some resolution of the wake. If the range resolution could be improved by a factor of five, then the wake could be dissected in a number of discrete sections.

A velocity spectrum could then be obtained for each section. These might look like the spectra sketched in Fig. 5(a-b). Except for the ambiguity in velocity, the spectra would resemble those sketched in Fig. 2.

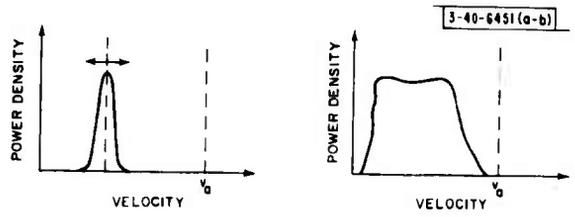

(a) Ronge segment including the RV.

(b) Ronge segment neor toil end of woke.

Fig. 5. Possible velocity distributions which moy be observed by o rodor system with ronge resolution ond hoving velocity resolution with velocity ombiguity ot multiples of v_o.

Consideration was then given to the possibility of increasing the repetition rate hy a factor of three and decreasing the pulse width to approximately 0.2 μsec (200 ft). If this could be achieved at a reasonahle cost and on a time scale which would make it possible to obtain data on trail turbulence considerably in advance of the summer of 1963, then it seemed well worth undertaking.

B. Modifications Needed to Improve the Range Resolution and Doppler Ambiguity of the UHF Radar at Wallops Island

In order to decrease the pulse width of a radar system to 0.2 μsec, a handwidth of at least 10 Mcps* is requircd in the following major components of the system:

(1) Microwave components, including the antenna and feed system, transmission-line system, duplexer, parametric amplifier and mixer,

(2) Transmitter,

(3) Receiver (IF and video),

(4) Data display and recording system.

The transmitter must be able to he switched with a rise time consistent with the pulse duration.

In order to increase the repetition rate to three times the normal operating value, the transmitter-modulator combination must be capable of operating at an increased value of average power.

In order to measure Doppler velocity, a receiving system is necessary which can measure phase as well as amplitude.

One of the most difficult aspects of the modification might have been the transmitter. An amplifier-transmitter is almost essential for the measurement of phase, but few of these exist with the appropriate bandwidth. Fortunately for this program, the Wallops Island UHF final amplifier was a copy of the Boston Hill broad-band UHF amplifier. It was fundamentally capable of broad-band operation, although it was not so operated at Wallops Island. None of the components associated with the transmitter, such as the duplexer and the driver, was designed for broad-band operation.

* To ollow for the possibility of utilizing 0.1-μsec pulses, on overoll bondwidth of 20 Mcps wos token to be on objective of the modificotion.

Such broad-band component designs had been developed for the Boston Hill radar, which had a 50-Mcps bandwidth, and therefore we were confident that the transmitter could be broadbanded to at least 20 Mcps. Transmission-line systems in waveguide or coaxial line are fundamentally broadband, provided that care is exercised in the choice of components and in assembly. Therefore, we were confident that, if the transmission-line system did not have the required characteristic, this could be remedied.

No information was available on the antenna and feed system. Since a combined frequency feed with dual polarization was in use, such a complex device could be a limiting item in obtaining the necessary bandwidth. A redesign of the feed might require considerable effort.

The RF amplifier in use at Wallops Island was a parametric amplifier constructed by Division 4. It did not have the requisite bandwidth, and therefore required replacement. As a result of our experience with broad-band parametric amplifiers, we were confident that a parametric amplifier of the required bandwidth could be provided.

The IF portion of the receiving, data-display, and recording systems following the RF amplifier required completely new units; thus they represented one of the major undertakings of the modification program. Because of our experience with similar designs for the TRADEX modification, these were considered a reasonable undertaking. A change in IF frequency from 30 to 60 Mcps was required in order to realize the necessary increase in bandwidth, and this entailed a replacement of the frequency synthesizer.

The Boston Hill UHF transmitter and modulator had been designed to operate in two modes: 300 prf at 6 μsec, and 1200 prf at 3 μsec. Therefore, no difficulty was anticipated in operating at a prf of 960, provided that the pulse width was no larger than 3 μsec.* Switching the modulator to generate a pulse as narrow as 0.2 μsec was out of the question. The driver, however, could be designed to deliver a 0.2-μsec RF pulse to the final amplifier. Although this involved a waste of modulator power, it was of no consequence, since the power capacity was already installed. With this approach, a continuously variable pulse width from 0.2 to 3.0 μsec could be provided.

In summary, the modifications and additions required seemed reasonable to undertake on a time scale which would ensure operation well in advance of the AMRAD or modified TRADEX radars. The cost did not appear to be great. The project was therefore undertaken upon receipt of a request from Dr. G. F. Pippert (of Group 37) dated 30 April 1962.

A number of Groups within the Laboratory contributed to this modification program:

Transmission lines	Group 46
Duplexer	Group 46
Parametric amplifier and mixer	Group 46
Transmitter driver	Group 46
Final amplifier and modulator	Groups 46 and 48
Synchronizer	Group 41
Frequency synthesizer	Group 41
Receiver (IF and video)	Group 41
Multiplex timing and sample-and-hold circuits	Group 47
Display and recording equipment	Group 47

* This onticipotion proved to be incorrect.

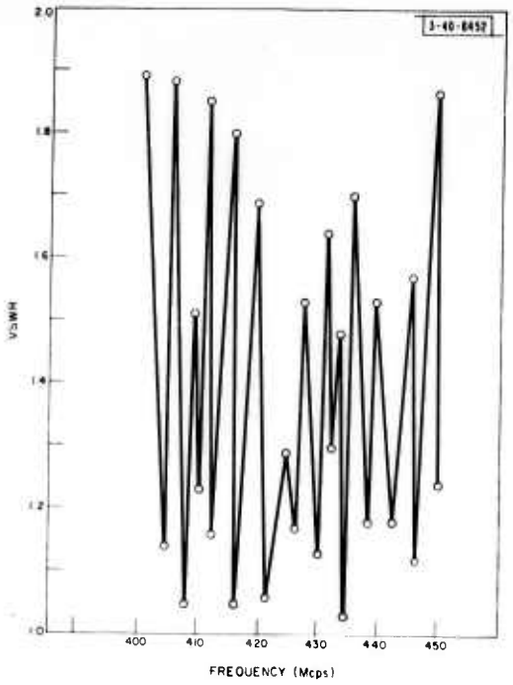

Fig. 6. VSWR vs frequency characteristic af UHF plumbing before modification to upgrade radar performance.

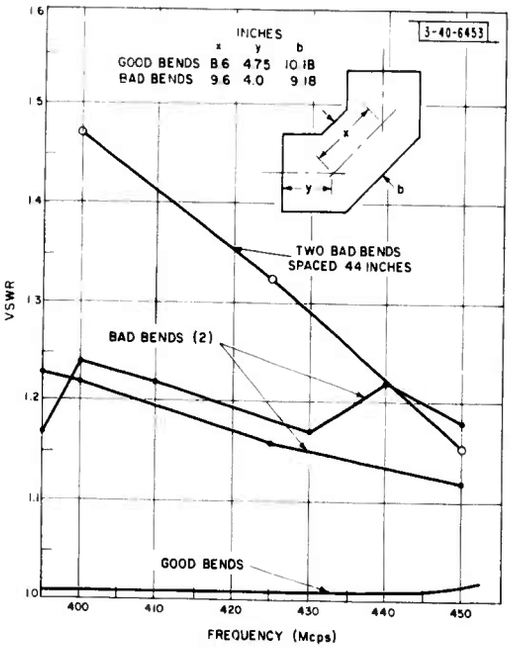

Fig. 7. Characteristics of good and bad E-plane bends used in the ariginal UHF waveguide installation.

The sections describing the details of the modification were contributed by the following staff members:

Transmission lines	C. W. Jones and W. A. Andrews
Duplexer	C. W. Jones and C. E. Muehe
Parametric amplifier and mixer	C. Blake
Transmitter driver	C. Blake
Final amplifier and modulator	E. Silverman
Synchronizer and frequency synthesizer	D. R. Bromaghim, W. H. Drury, and A. A. Galvin
Receiver (IF and video)	S. Spoerri
Multiplex timing and sample-and-hold circuits	D. F. Mayer
Display and recording equipment	J. P. Perry

II. MICROWAVE COMPONENT MODIFICATIONS

The modifications to the microwave components of the UHF radar are described in three sections:

Transmission Lines,
Duplexer,
Parametric Amplifier and Mixer.

The transmission line and antenna feed system initially had a poor voltage-standing-wave-ratio (VSWR)-vs-frequency characteristic. Fortunately the feed system had an acceptable, if not desirable, VSWR characteristic. The remainder of the transmission line was rebuilt to provide good performance. The combined transmission line and feed characteristic are now acceptable.

The duplexer system was replaced with a broad-band duplexer.

The parametric amplifier was replaced with a new amplifier having broad-band characteristics and improved noise temperature.

A. Transmission Lines

The transmission system consists of two lines from the antenna feed to the transmitter and receiver rooms. The line carrying the transmitter power is in WR-2100 waveguide and the line bringing down the orthogonally polarized received signal is in 3-1/8-inch rigid coaxial line and 7/8-inch heliax. These two systems are assemblies of conventional straight sections, bends, flexible sections, plus azimuth and elevation rotary joints similar to those at Millstone Hill and at Boston Hill. In addition, each of these transmission lines originally incorporated a tuning mechanism for refining the match in the narrow-frequency band that was being used.

The VSWR characteristic of the original waveguide transmission system is plotted in Fig. 6. From the nature of the variations of the VSWR over the range of measurement, one can infer that the characteristic is principally due to a small number of mismatches separated by many wavelengths. The troublesome components were isolated by breaking the plumbing at several points and measuring the VSWR. It was found that there were four E-plane bends which were dimensionally incorrect and that these bends were responsible for most of the mismatch of the waveguide system. Figure 7 depicts the VSWR characteristic of the good and bad bends. Figure 8 shows two of the bad bends in the original installation in the transmitter room. The UHF high-power feed assembly is shown in Fig. 9. The VSWR of this assembly, measured looking into the

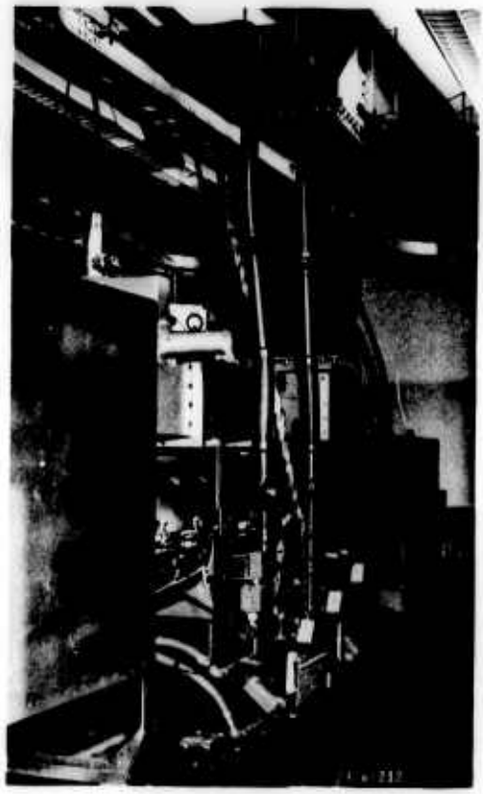

Fig. 8. Transmitter, showing narraw-band branching duplexer above the VA-812C klystron. Twa af the bad E-plane bends which were removed fram the system are shawn in the waveguide run above the klystron.

Fig. 9. Antenna, showing UHF waveguide run down to the reor of the dish and the heliax coble which carries the arthogonal polarizotian received signol.

E-plane mitered bend, is plotted in Fig. 10. This E-plane bend at the base of the feed assembly was not measured for VSWR separately, because this would have required complete disassembly of the feed due to the nature of the feed-support mechanism. The bend was given a dimensional check and was within the tolerance for good bends. The VSWR characteristic of the feed assembly was considered adequate, although there was a higher-than-desired VSWR peak at band center. To make any significant improvement in the feed would probably require a major modification, if not complete redesign, and was not considered practical at this time.

The VSWR of the orthogonal polarized receive channel (Fig. 11) was quite bad, but could be corrected to some extent by means of a transformer section. Further improvement did not seem possible with that particular feed design. The orthogonal UHF feed and the X-band horn are shown in Fig. 12. The feed assembly viewed from the outside is shown in Fig. 13.

The coaxial line from the orthogonal feed to the receiver was considered adequate, although about 0.5-db improvement in insertion loss was possible if the 7/8-inch heliax were to be replaced by 3-1/8-inch rigid coaxial line. Present orthogonal line losses ignoring the monoplexer are:

90 feet of 7/8-inch heliax	0.81 db
100 feet of 3-1/8-inch rigid coax	0.24 db
Total line loss	1.05 db

The only modification to the orthogonal line was to remove the tuner, since this component was unnecessary when the feed VSWR was reduced by a 5:1 ratio dielectric transformer placed a half-wave from the dipole.

The performance of the UHF waveguide transmission system is plotted in Fig. 14. When the bad bends were replaced, the residual VSWR was essentially that of the feed assembly in the 400- to 450-Mcps band and was considered adequate for good performance under short-pulse operation.

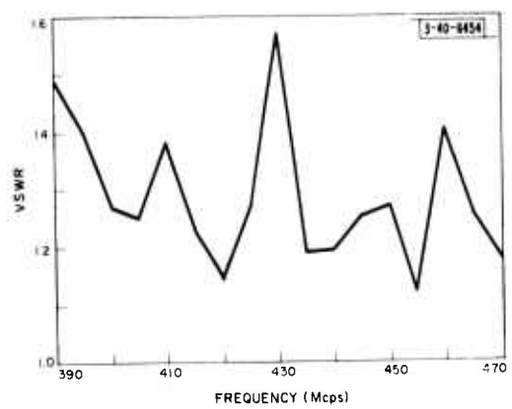

Fig. 10. VSWR-vs-frequency chorocteristic of UHF ontenno feed horn meosured at the rear of the dish.

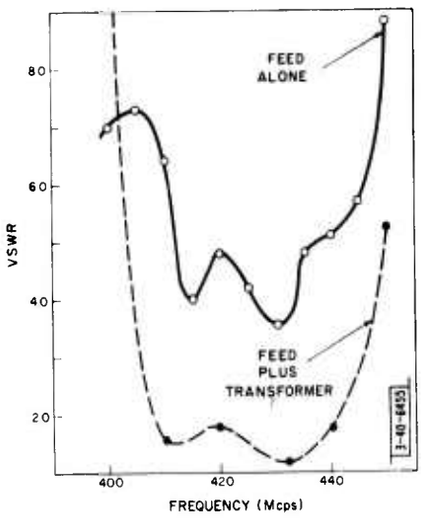

Fig. 11. VSWR characteristic of orthogonol UHF feed before and ofter installotion of quorter-wovelength motching tronsformer.

Fig. 12. Orthogonal UHF feed assembly and X-band horn looking toward the aperture of UHF horn. The face of the UHF horn is covered with a sheet of dielectric material which acts as a weather seal. The X-band horn protrudes through this dielectric plate.

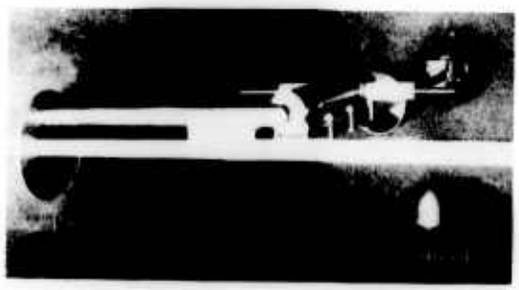

Fig. 13. Feed assembly of UHF radar, showing X-band horn in the center of the UHF aperture and the connection to the UHF orthogonal feed coaxial line near the base of the UHF horn.

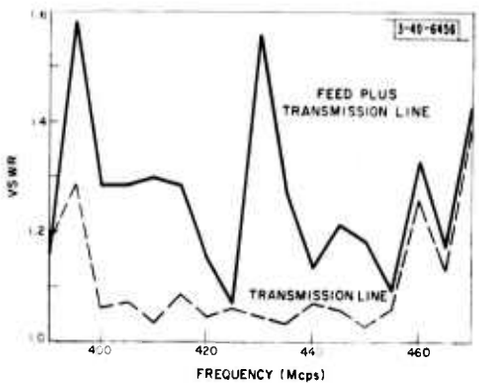

Fig. 14. VSWR characteristic of UHF waveguide system from the duplexer to the antenna. The solid lines show the complete system, including the horn characteristic. The dashed line is the transmission-line characteristic measured to the rear of the dish.

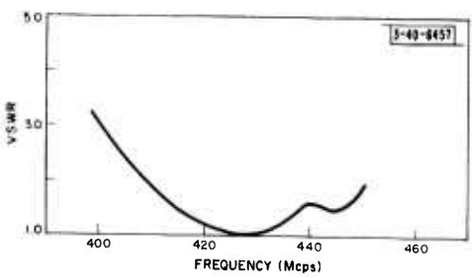

Fig. 15. VSWR characteristic of orthogonal feed and transmission line as measured at the receiver.

The characteristic which was achieved for the combination of the orthogonal line and the orthogonal feed is shown in Fig. 15. The measured characteristic of the transmission line between the receiver and the input to the orthogonal feed at the UHF horn is depicted in Fig. 16. The measured attenuation matches the calculated value of 1.05 db within the accuracy of the measurement, except at the low-frequency end where there is an unexplained high-loss point. Since this is outside the operating band of 420 to 450 Mcps, it was not investigated.

B. Duplexer

The duplexers originally used in the UHF radar were designed for narrow-band operation; consequently, it was necessary to replace them with suitable broad-band components in order to convert the radar to short-pulse operation. The branching duplexer in the main line was replaced hy a Bomac Lahoratories (BL-P-011D) halanced duplexer and the high-Q, single-tuned monoplexer in the orthogonal line was replaced by a Metcom double-tuned circuit. Both these units employ gas discharge tubes as the active elements.

The BL-P-011D duplexer is a modified commercial version of the broad-band duplexer developed at Lincoln Laboratory for use at Boston Hill. Its characteristics are given below.

Bandwidth	420 to 450 Mcps
Peak power (min)	15 Mw (6-μsec pulse)
Average power (min)	120 kw (6-μsec pulse)
Receiving VSWR (max)	1.2
Receiving insertion loss	0.6 dh max
Recovery time	200 μsec
Flat leakage (max)	10 watts peak (6-μsec pulse)
Spike leakage (max)	1000 ergs

As measured at the site, the VSWR and insertion loss were within the specifications (Fig. 17). At a peak power of 6 Mw, using a 1-μsec pulse, the peak leakage was 4 watts. With a 6-μsec pulse, the peak leakage was 1 watt. The minimum discernible signal through the duplexer and receiver was 111 dbm for the 1-μsec pulse and 115 dbm for the 6-μsec pulse. The transmitting VSWR of the duplexer is very low, but was not measured separately.

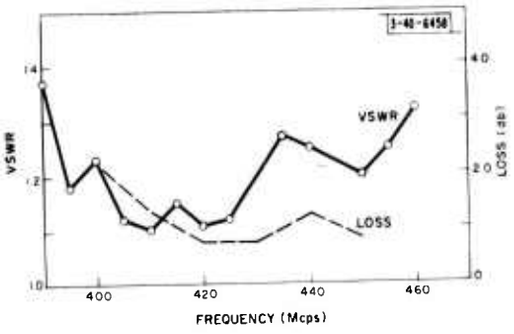

Fig. 16. Measured VSWR and insertian lass characteristic af arthaganal transmissian line.

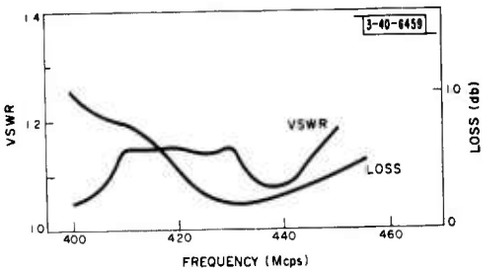

Fig. 17. VSWR and insertian lass an receive af the BL-P-011D duplexer after installatian at Wallaps Island.

The Metcom double-tuned monoplexer is built in 3-1/8-inch coaxial line and employs two gas tubes, MTT-17a and MTT-13. These are similar and interchangeable with the BL-931 and BL-994, respectively, used in the main duplexer. The specifications of this unit are:

Bandwidth	400 to 450 Mcps
VSWR (max)	1.5
Insertion loss (max)	0.5 db
Recovery time	100 μsec
Peak incident power	100 kw (max) at 6-μsec pulse, 300 prf
Leakage (max)	5 watts peak

The measured VSWR and insertion loss characteristics are plotted in Fig. 18.

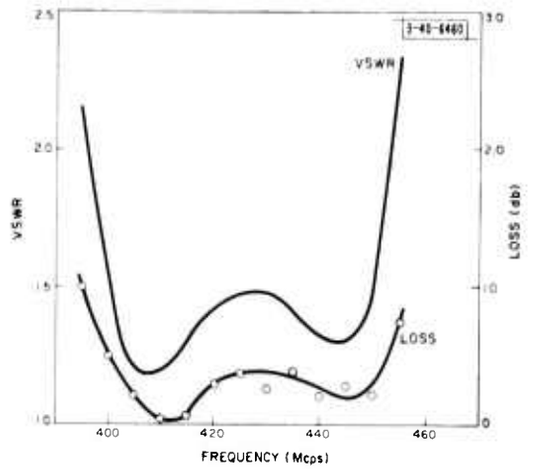

Fig. 18. VSWR and insertion loss on receive of the Metcom monoplexer.

The duplexer and monoplexer were standard commercial items and, although not designed for short-pulse operation, were believed to be adequate for the Wallops Island application. Since there was no source of high-power RF capable of less than 1-μsec pulse length available for testing these units, it was not possible to complete their evaluation before installation at the site. Although their use was somewhat of a gamble, the design, development, and testing of components specifically for this application would have taken several months and would have exceeded any acceptable time scale.

The amplitude of the spike on the duplexer leakage envelope is a function of the rate of rise of the applied high-power RF pulse, as well as of the ionization potential of the gas used in the TR tubes. It was feared that the rate of rise of the short pulses to be used in the upgraded Wallops Island system might be sufficiently greater than the rate of rise for which the duplexer had been tested to increase the spike amplitude to a point where the parametric amplifiers would be damaged. The system was operated in the short-pulse mode and the leakage envelope observed on a fast oscilloscope. No significant increase in spike amplitude was observed and no difficulty was experienced with the performance of the receivers. As an added precaution, however, solid

state limiters, having an insertion loss of 0.25 db, were placed directly in front of the receiver. These can withstand short pulses of the order of a kilowatt peak and have a limit level of a few watts peak. At this writing, only a very limited amount of operating time has been accumulated in the short-pulse mode but, judging from the limited data, the duplexer appears to be functioning satisfactorily.

C. Parametric Amplifier and Mixer

Two receivers are required in the Wallops Island UHF system: one for direct or vertical polarization, and one for orthogonal or horizontal polarization. The antenna temperature is sufficiently low and the losses between it and the receivers are sufficiently small to justify considerable effort in achieving low-noise reception. The receivers in the original system were good noise-wise, but would have required extensive modification before they would have met all the requirements of the upgraded system. These receivers were designed before high-quality circulators were available and were originally operated without them. However, the stability of the original receivers improved markedly when circulators, employed in this case as isolators, were introduced in the inputs. Circulators were therefore added, once they became available.

The upgraded receivers reflect the recent advances made in the technology of parametric amplifiers and ferrite circulators. Although the same basic components are used, the upgraded receivers are much smaller, have larger gain-bandwidth products, and are considerably more stable than their predecessors. They are also simpler to align, require less attention, and have lower excess noise temperatures.

1. Original Receivers

The original receivers were varactor-diode, four-frequency up-converters. These units were pumped at 5980 Mcps. Signal energy at 425 Mcps was amplified and frequency translated to 6405 Mcps. If energy at only these three frequencies (425, 5980 and 6405 Mcps) were to interact with a nonlinear reactance (varactor), the maximum gain would be only 6405/425. Additional gain was obtained at some sacrifice of bandwidth, stability, and simplicity by supporting a fourth frequency (5555 Mcps) as an idler. Figure 19 shows the original receiver with its associated power supplies, pump, and the circuitry for obtaining a coherent 30-Mcps IF output signal. A complete description of the receiver is given by Parsons, et al.* Table I is a summary of the amplifier characteristics.

Each up-converter was followed by an LEL Model MCC-3 mixer-IF preamplifier integrated assembly. The system local oscillator (LO) (395 Mcps) was combined with the pump (5980 Mcps) in a high-level mixer which uses a 1N21E diode. The sum frequency (6375 Mcps) was extracted for use as the LO for the MCC-3 mixer. In this manner, signal-phase coherence was preserved with the system master oscillator or stalo.

2. Upgraded Receivers

The parametric amplifiers now in use are the more conventional 1-port regenerative type. The gain-bandwidth product of these amplifiers is greater than the gain-bandwidth product of the up-converters, but the bandwidth requirements of the upgraded system are too large to obtain all the needed low-noise gain in a single stage. The problem is resolved by following the parametric

* A. Parsans, E. P. McCurley and C. Blake, "An Operational UHF Reactance Amplifier," Praceedings, Symposium an the Applicatian af Low-Naise Receivers to Radar and Allied Equipment, Lincaln Laboratory, M. I. T. (Navember 1960), Val. III.

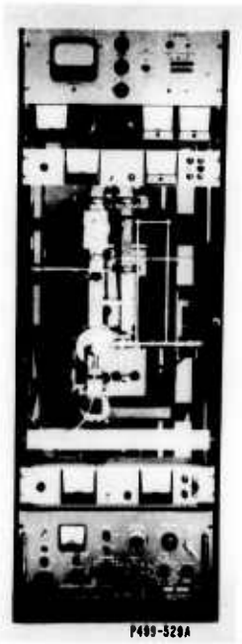

Fig. 19. Faur-frequency up-canverter and its assaciated equipment.

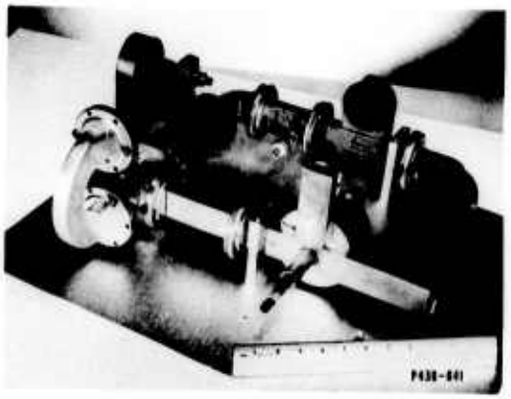

Fig. 20. One-port parametric amplifier.

TABLE I CHARACTERISTICS OF THE FOUR-FREQUENCY UHF PARAMETRIC UP-CONVERTER	
Input frequency	425 Mcps
Output frequency	6405 Mcps
Excess naise temperature	150°K
Gain	26 db
Bandwidth	10 Mcps

TABLE II CHARACTERISTICS OF THE ONE-PORT UHF PARAMETRIC AMPLIFIER	
Input frequency	420 Mcps
Output frequency	420 Mcps
Excess naise temperature	80°K
Gain	16 db
Bandwidth	30 Mcps

amplifier with a low-noise transistor amplifier. The new amplifiers use the same basic components as did the old up-converters. Few new components were required that would not have been necessary anyway in order to upgrade the original receivers. A pump-power regulating feature has been added to the new amplifiers. This regulator consists of a pump coupler and detector, a differential DC amplifier, and a diode attenuator. These components form a feedback loop such that when pump power increases, the detector current increases; this increase is amplified by the DC differential amplifier which, in turn, drives the diode attenuator into a region of greater attenuation, therehy tending to restore the pumping level. When pump power decreases, the mechanism is reversed. With this arrangement, variations of pump power from the klystron of ±2 db cause amplifier gain variations of less than ±0.2 db.

The 1-port parametric amplificr is shown in Fig. 20, and its characteristics are given in Table II. Broadbanding of this amplifier is accomplished by operating at a reduced gain, as mentioned above, and through the use of a double-tuned input circuit. The secondary of this circuit is the original signal cavity. The primary is a commercial double-slug tuner. The frequency response of this unit for a gain of 16 db is shown in Fig. 21.

Figure 22 is a block diagram of the complete upgraded front end. A Micro State Model L-202 limiter provides 35 db of isolation from any TR spike leakage that might otherwise be incident upon the parametric amplifier. Two 3-port circulators provide isolation of the input and output of the amplifier. The transistor RF amplifier adds 27 db to the receiver gain. Since the gain of the parametric amplifier is 16 db, the transistor amplifier with its excess noise temperature of 600°K contributes 15°K to the effective noise temperature referred to the input to the parametric amplifier. The effective noise temperature of the system is improved by about 1.5 db over the original system. The output impedance of the transistor amplifier is very high and the balanced mixer that follows it is quite sensitive to impedance mismatches. The two are therefore isolated by a 6-db pad. The net receiver gain at this point is sufficiently great that no measurable degradation of noise performance is introduced by this loss.

The mixer-IF preamplifier uses the original IF amplifier rewired for a 20-Mcps bandwidth and a 60-Mcps center frequency. The C-band balanced mixer has been replaced with a UHF unit. The gain from the mixer RF input to the IF output is 20 db. The new mixer-IF amplifier excess noise temperature is a rather high 6000°K; but, with 36 db of gain in front of it, this high value is quite tolerahle and justifiahle. The mixer begins to saturate or compress at an input level of −20 dbm and thereby establishes the upper limit of the dynamic range of the

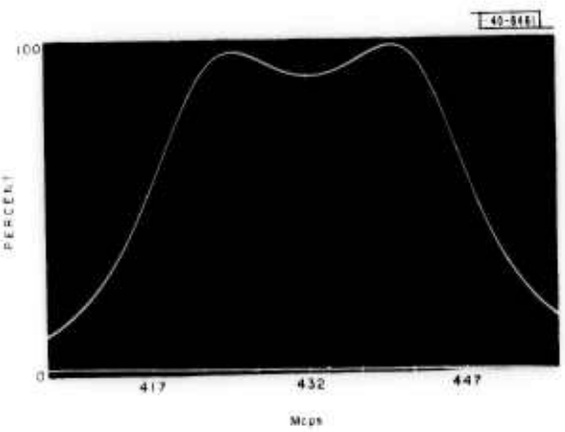

Fig. 21. Frequency response of 1-port parametric amplifier. Amplifier gain is 16 db and horizontal scale is 5 Mcps/div.

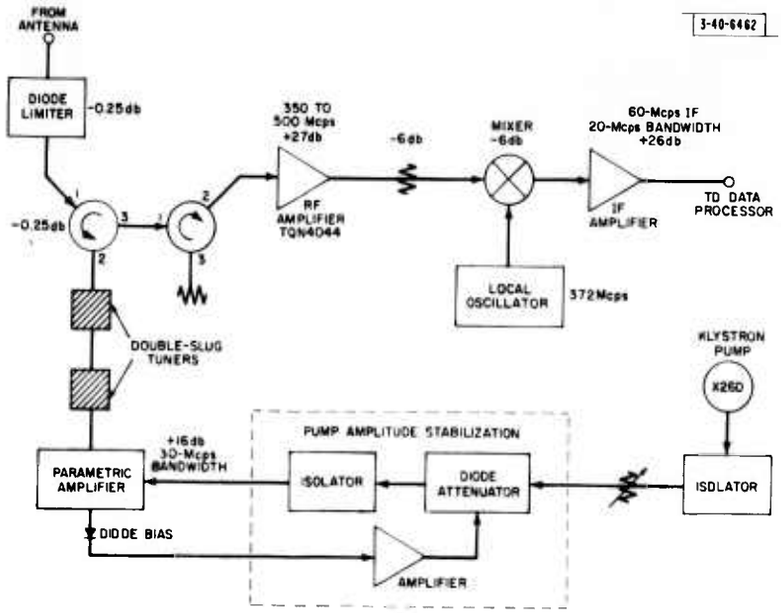

Fig. 22. Block diagram of upgraded UHF front end.

TABLE III CHARACTERISTICS OF THE COMPLETE UPGRADED RECEIVER	
Input frequency	420 Mcps
Output frequency	60 Mcps
Excess noise temperature	100°K
Over-all gain	56 db
Over-all 3-db bandwidth	20 Mcps
Input saturation level	−56 dbm
Maximum allawable spike leakage	1250 watts

entire system. Since there is 36 db of gain ahead of the mixer, the system saturation level is −56 dbm. Table III summarizes the performance of the complete receiver. The IF preamplifier with its 20-Mcps bandpass is the bandwidth limiting component in the system.

3. Receiver Alignment

The broad-hand requirements of the upgraded system make it mandatory that the receiver be aligned with a swept-frequency oscillator. The Telonic Industries, Inc., Model PD-8 has been procured for this purpose. Re-alignment should be necessary only in the event of a diode burnout. In such an event, the probability is high that the diode limiter and the transistor RF amplifier have also been damaged; hence, these units should be checked. Burnout should not occur unless the TR leakage has exceeded 1250 watts peak.

To align the parametric amplifier, the equipment is connected as described in Fig. 23. The level at the input to the parametric amplifier must not exceed −40 dbm. It is therefore necessary to use an oscilloscope with a sensitivity of at least 10 mv/cm. A good detector should also be used – one with a tangential sensitivity of at least −50 dbm.

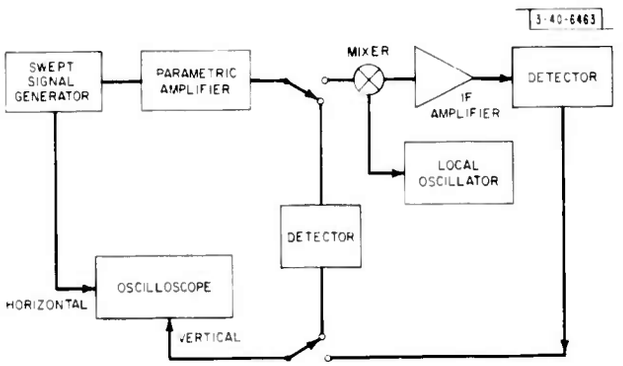

Fig. 23. Equipment arrangement for aligning parametric amplifier.

The detector does not need to have matching pads in front of it, but if a 6- or 10-db pad can be tolerated, it would do no harm to use it. The varactor-diode bias voltage should be set at 0.7 volt. The pump level should be set such that the diode forward current is 5 μa. A double-tuned response curve similar to Fig. 21 can then be obtained by adjusting the double-slug tuner, the micrometer, and the waveguide plungers. Trimming adjustments of the bias, pump power, and pump frequency are permissible, but usually are not required.

The receiver components following the parametric amplifier can be checked out stage-by-stage. The detector is simply moved to the output of each successive stage as it is cascaded in the normal operating fashion. Care should be taken to keep the input level low enough so that all the stages operate in a linear region. No provision has been made to flatten the response of these units. Small corrections can be made by trimming the alignment of the parametric amplifier.

III. TRANSMITTER MODIFICATIONS

The modifications to the transmitter are described in three sections:

The Transmitter Driver
The Final Amplifier and Modulator
The Synchronizer.

TABLE IV ORIGINAL TRIODE DRIVER CHARACTERISTICS	
Center frequency	425 Mcps
Input power level	50 mw
Peok output power level	500 wotts
Bandwidth	5 Mcps
Plote pulse	3 kv, 10 amp
Plote pulse durotion	1 to 10 μsec
Pulse repetition rote	320 pps

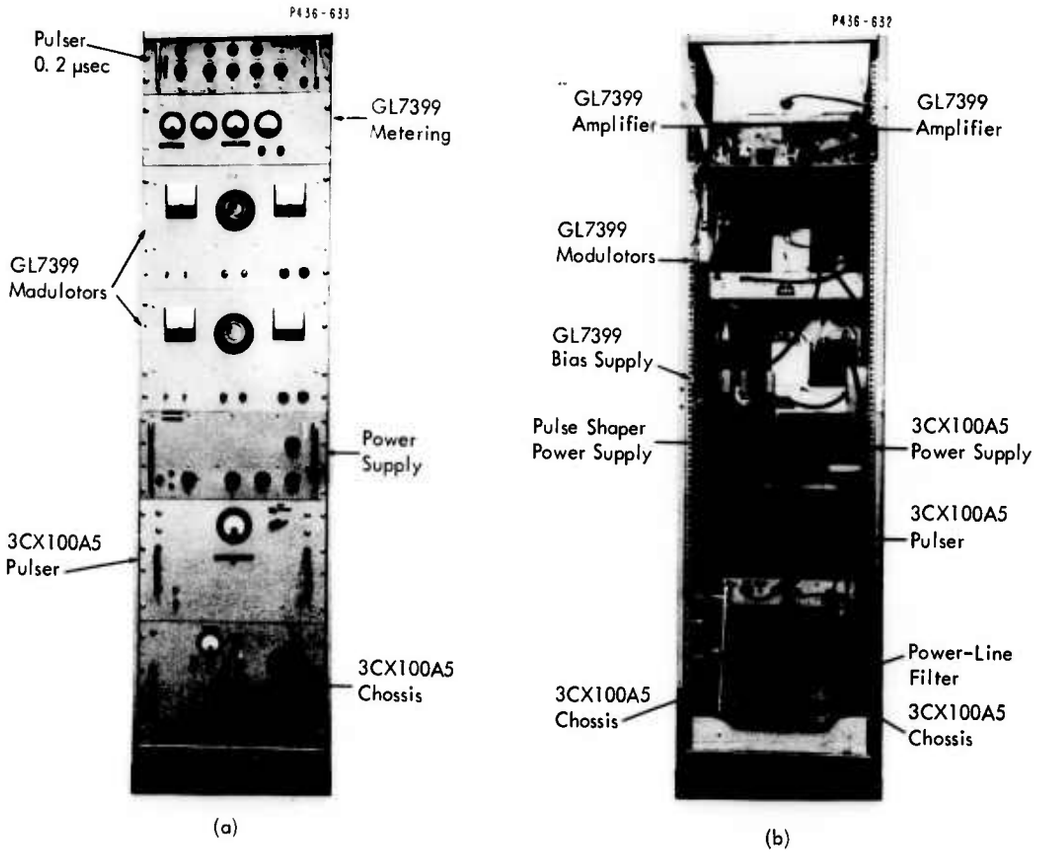

Fig. 24. Driver system.

The driver was modified to provide an RF pulse to the final amplifier which is variable in width from 0.2 to 3.0 μsec.

The final amplifier was modified to have an RF bandwidth of 40 Mcps, more than adequate to reproduce faithfully a 0.2-μsec pulse. The modulator was modified to permit reliable operation at a pulse repetition frequency of 960.

The synchronizer was replaced with a unit which could provide the necessary timing to the UHF and S-band radar at both 320 and 960 pps.

The details of the modifications are given in the sections which follow.

A. Transmitter Driver

In both the original and the upgraded UHF radar, the transmitter driver performs two functions: (1) it amplifies the low-level signal from a few milliwatts (output of the frequency synthesizer) to a power level sufficient to drive the VA-812C high-power klystron, and (2) it shapes the RF signal into an approximately rectangular pulse. The duration and rise and fall times of the pulse are preserved as the signal proceeds through the transmitter components following the driver.

The original system bandwidth requirements permitted high-gain, narrow-band alignment of the VA-812C klystron. In this mode of operation, 100 watts of drive power comfortably saturated the VA-812C. In the new mode of operation, a low-gain, broad-band alignment of the VA-812C klystron must be employed and 10 kw of drive are needed to assure adequate klystron saturation. The original driver is incapable of operating at this power level.

In the original system, the pulse duration was established by the driver modulator and could be varied continuously from about 2 to 6 μsec. The rise and fall times of this pulse were several hundred nanoseconds and the system bandwidth was adequate to pass this pulse with little degradation of the pulse shape. In the upgraded system, pulse duration is determined by a commercial pulse generator (E-H Model 131). This unit provides video drive to the pulse shaper. A single knob on the front panel of this pulse generator allows the pulse duration of the radiated signal to be adjusted continuously from 0.2 to 3.0 μsec. The rise and fall times of the envelope of the radiated RF pulse must not exceed a few tens of nanoseconds. This requirement is met by having 30-Mcps passbands in all components through which the pulse passes.

1. Original Driver

The original driver, hereafter referred to as the triode driver, is described in detail in Lincoln Laboratory Report 21G-0011 [U] by B.G. Kuhn.* The triode driver consists of a cascade of four grounded-grid triodes (3CX100A5). These stages can be synchronously tuned for high-gain, narrow-band operation, or can be stagger-tuned for low-gain, broad-band operation. The driver requirements of the original system were narrow band and high gain, and the unit was aligned accordingly. The performance characteristics were roughly as shown in Table IV.

The triode driver uses a conventional, hard-tube modulator that provides up to a 3-kv pulse for the anodes of the four triodes. The power supply for this modulator is a slightly modified commercial unit. The bottom three panels of Fig. 24 are the triode driver. Details of the modulator are also given in Kuhn's report.

---

* ASTIA 244586, H-182.

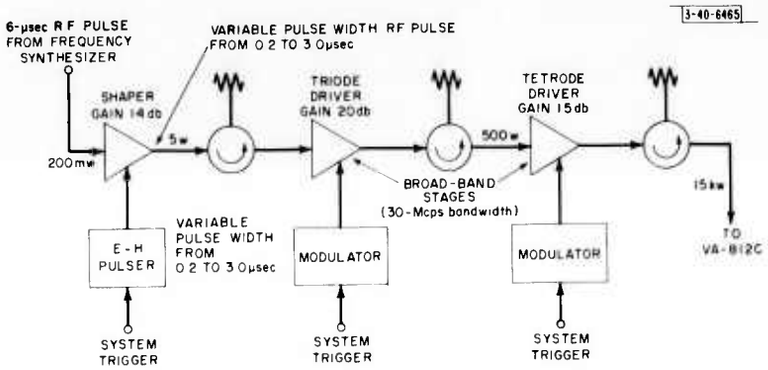

Fig. 25. Block diagram of driver system.

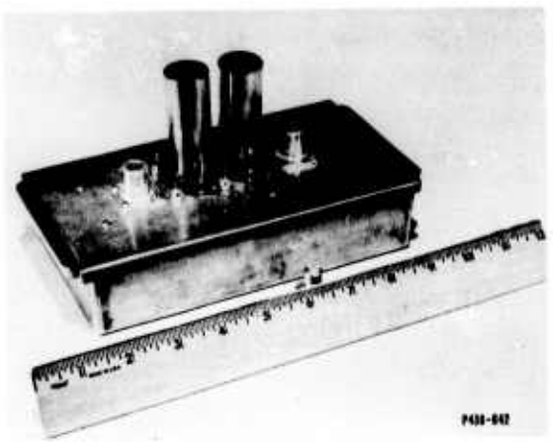

(a)

(b)

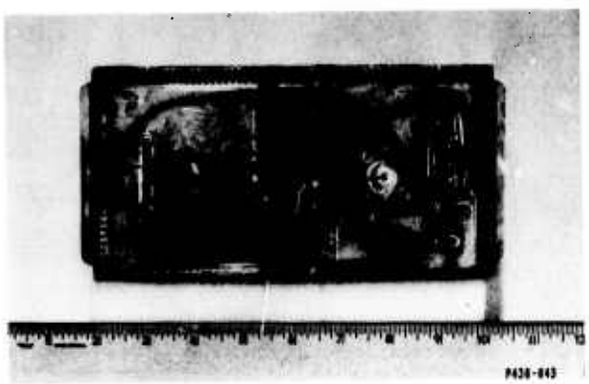

Fig. 26. Pulse shaper.

2. Upgraded Driver System

The upgraded driver system is a cascade of three amplifying units: (a) a pulse shaper, (b) the original triode driver, and (c) a tetrode driver. The gross characteristics and functions of these units are indicated in Fig. 25. The pulse shaper gates a short-duration, fast-rise-time, RF pulse from a low-power-level (200 mw), long-duration pulse. It also amplifies this pulse to the 5-watt-peak level. The triode driver, now aligned for broad-band operation, amplifies this pulse from 5 to 500 watts. Finally, the tetrode driver increases this level to a 15-kw peak. Figure 24(a-b) displays the rack containing this equipment.

3. Pulse Shaper

The pulse shaper consists of a cascade of two gated 6939 tetrodes. Figure 26 shows an overall and an interior view of this unit. Figure 27 is the wiring diagram and Fig. 28(a-c) displays the RF pulses obtained from this unit at 3 different pulse width settings. There is a pronounced ringing on the leading edge of these pulses. The frequency of this ringing is 100 Mcps which places it well outside the 15-Mcps video passband of the system. It is possible to reduce the video drive level and largely suppress this ringing, but in so doing, the pulse shaper performance becomes sensitive to the video pulse amplitude and shape. It is recommended that the video pulse be 50 volts and that the ringing be tolerated. The ringing is effectively filtered out by the components which follow the pulse shaper; with this ringing included, the pulse shaper has the characteristics given in Table V. The pulse duration is continuously adjustable from 0.2 to 3 μsec. The duration is controlled by a single knob control on the front panel of the E-H Model 131 pulser.

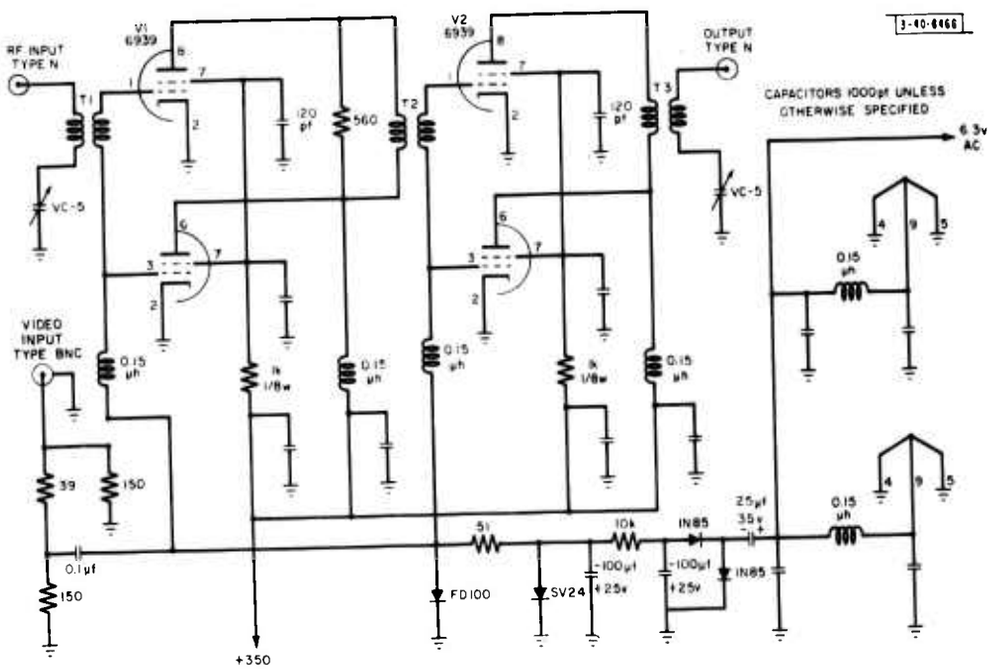

Fig. 27. Wiring schematic of pulse shaper.

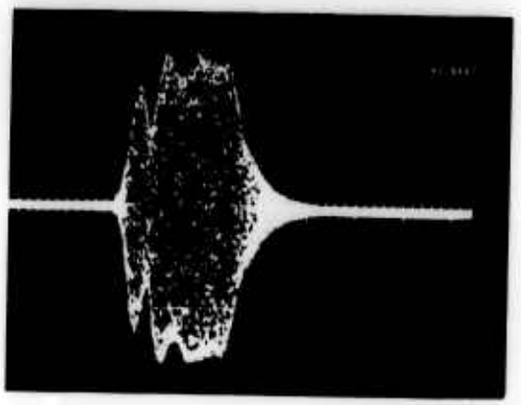

(a) Sweep rate, 20 nsec/div.

(b) Sweep rote, 20 nsec/div.

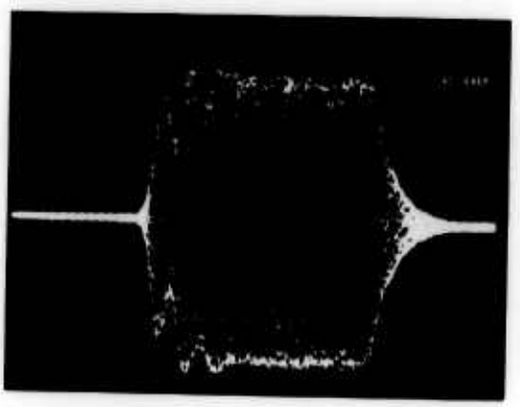

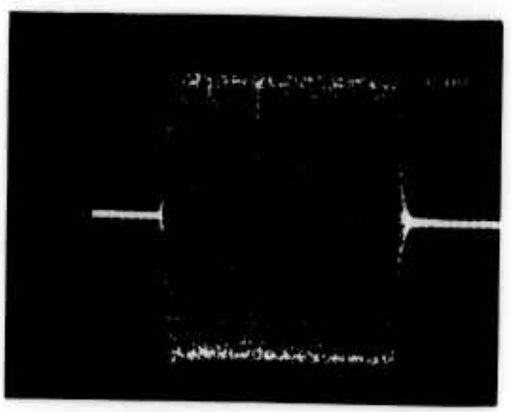

(c) Sweep rote, 100 nsec/div.

Fig. 28. Sompling oscilloscope presentotion of pulse shoper output. Pulse level, 5 wotts peok.

TABLE V CHARACTERISTICS OF PULSE SHAPER	
Input	CW or a brood pulse
Input level for soturoted operotion	200 mw
Center frequency	420 Mcps
Soturoted peok output level	5 wotts
Rise time, ten 90% points	25 nsec
Foll time, ninety 10% points	25 nsec
Isolotion	70 db
Video drive	+50 volts
Video impedonce level	50 ohms
Pulse durotion	0.2 to 3.0 μsec
Pulse repetition rote	320 or 960 pps

The power supply for the pulse shaper is a General Radio Model 1204B unit. Both the power supply and the pulse shaper are located in the rear of the driver rack behind the triode driver power supply.

4. Triode Driver

Essentially no modifications were made to the triode driver other than to align it for broad-band low-gain operation. Table VI summarizes its characteristics as operated in the upgraded system.

The rectangular RF pulses from the pulse shaper are timed to occur near the center of the 6-μsec pulses applied to the anodes of the triode driver. The proper timing is maintained through the use of adjustable time delay circuits in the triggering-pulse distribution system. This same technique is used throughout the radar system to assure correct time sequencing of all pulse processing.

TABLE VI TRIODE DRIVER CHARACTERISTICS IN THE UPGRADED SYSTEM	
Center frequency	420 Mcps
Peok input power level	5 wotts
Peok output power level	500 wotts
Bondwidth	30 Mcps
Plote pulse	3 kv, 10 omp
Plate pulse durotion	6 μsec
RF pulse durotion	0.2 to 3 μsec
Pulse repetition rate	320 or 960 pps

5. Tetrode Driver

The tetrode driver consists of two GL-7399, air-cooled, grounded-grid, tetrode amplifiers. The input or cathode circuitry is fabricated from flat metal strips on a micarta dielectric sheet in a manner not unlike triplate. The output circuitry is a rectilinear $\lambda/2$ TEM cavity. The outer conductor of this cavity is the box which houses the amplifier. The inner conductor is a piece of S-band waveguide with a hole at one end through the broad face of the waveguide that accepts and makes electrical contact with the anode of the GL-7399. At the other end of this waveguide there is an adjustable metal plunger that can be moved to shorten or lengthen the waveguide, and thereby tune the anode circuit. Figure 29(a-h) shows this unit with the covers removed. Working drawings (S-14392) are on file in the Lincoln Laboratory drafting room. These units were designed for and used in the electronic scanning array radar (ESAR) UHF program. They became surplus when the ESAR program emphasis shifted to L-band and the units were obtained as surplus government-furnished equipment for the upgraded Wallops Island UHF system. The drawings on file include some minor modifications required for this particular application. The original design was intended to operate with a 30-μsec pulse, whereas in this application, it was necessary to operate with a 3-μsec pulse. To preserve reasonable rise and fall times of this 3-μsec pulse, the plate

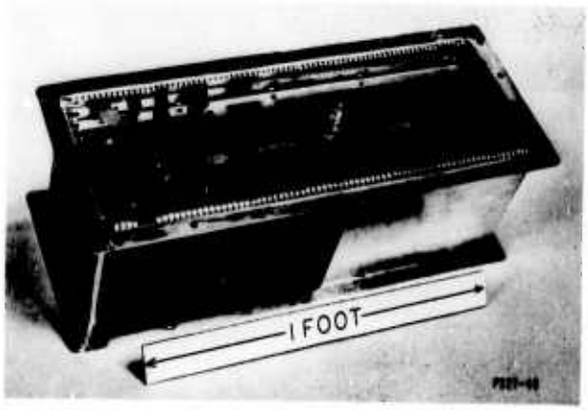

(a) Input or cathode circuitry.

(b) Output or anode circuitry.

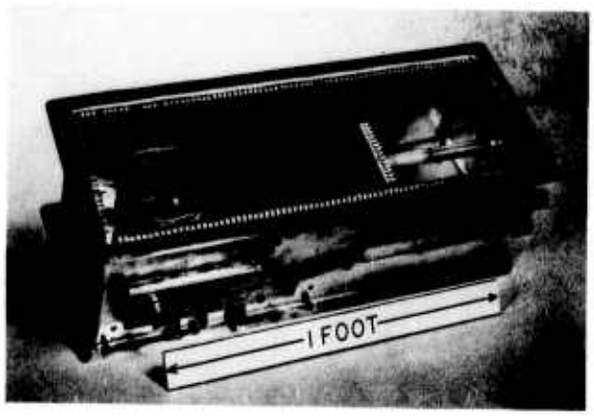

Fig. 29. Inside the tetrode driver.

and screen bypass capacitances at video frequencies were reduced from 300 and 250 pf, respectively, to 50 and 75 pf, respectively. Additional components were introduced into the screen and control-grid circuits to eliminate parasitic oscillations.

The two modulators for the tetrode stages were designed and built by Raytheon Manufacturing Company. Figure 30 is a circuit diagram of these modulators. They are of conventional line-pulser design, and use a 4C35 hydrogen thyratron as a switch tube. Table VII summarizes the characteristics of the tetrode driver.

The output of the tetrode driver connects to the No. 1 port of a circulator. The No. 2 port of this circulator connects to the VA-812C, and the No. 3 port is terminated with a 50-ohm load having a capacity of 25 kw peak, 500 watts average. This arrangement permits the 812C to present a completely reactive or reflecting termination without damaging the driver, since all reflected energy is dissipated in the load. Under some conditions of misalignment, the 812C may oscillate and power may be propagated toward the driver. This power is also harmlessly dissipated in the load connected to the No. 3 port of the circulator.

The ESAR cavities were designed for broad-band operation. The circuitry at both input and output is double tuned. The input circuitry is fixed, but the output primary tuning, secondary tuning, and coupling are all adjustable.

6. Driver System Alignment

The procedure for accomplishing and/or verifying broad-band operation of the complete driver system is depicted in Fig. 31. A swept-frequency oscillator (Telonic Model PD-8) has been procured which has a sufficient output power to drive the triode driver directly. The PD-8 sweeps linearly in frequency at a 60-cps rate. The driver system is pulsed at 960 pps. There is no phase lock between these two sources. Detectors connected to directional couplers at points along the system detect energy at a 960-pps rate. These samples represent the passband response as it is being swept at the 60-cps rate. Since the sources are not phase locked, the sample points drift, over a long period of time, so that they include all points in the frequency response curve. Figure 32(a-c) shows these curves as they were taken at the output of the triode driver, tetrode driver, and VA-812C, respectively.

TABLE VII
TETRODE DRIVER CHARACTERISTICS

Center frequency	420 Mcps
Peak input power level	500 watts
Peak output power level	15 kw
Bandwidth	30 Mcps
Plate pulse	9 kv, 10 amp
Screen pulse	2 kv, 0.5 amp
Plate and screen pulse duration	3 μsec
RF pulse duration	0.2 to 3 μsec
Pulse repetition rate	320 or 960 pps

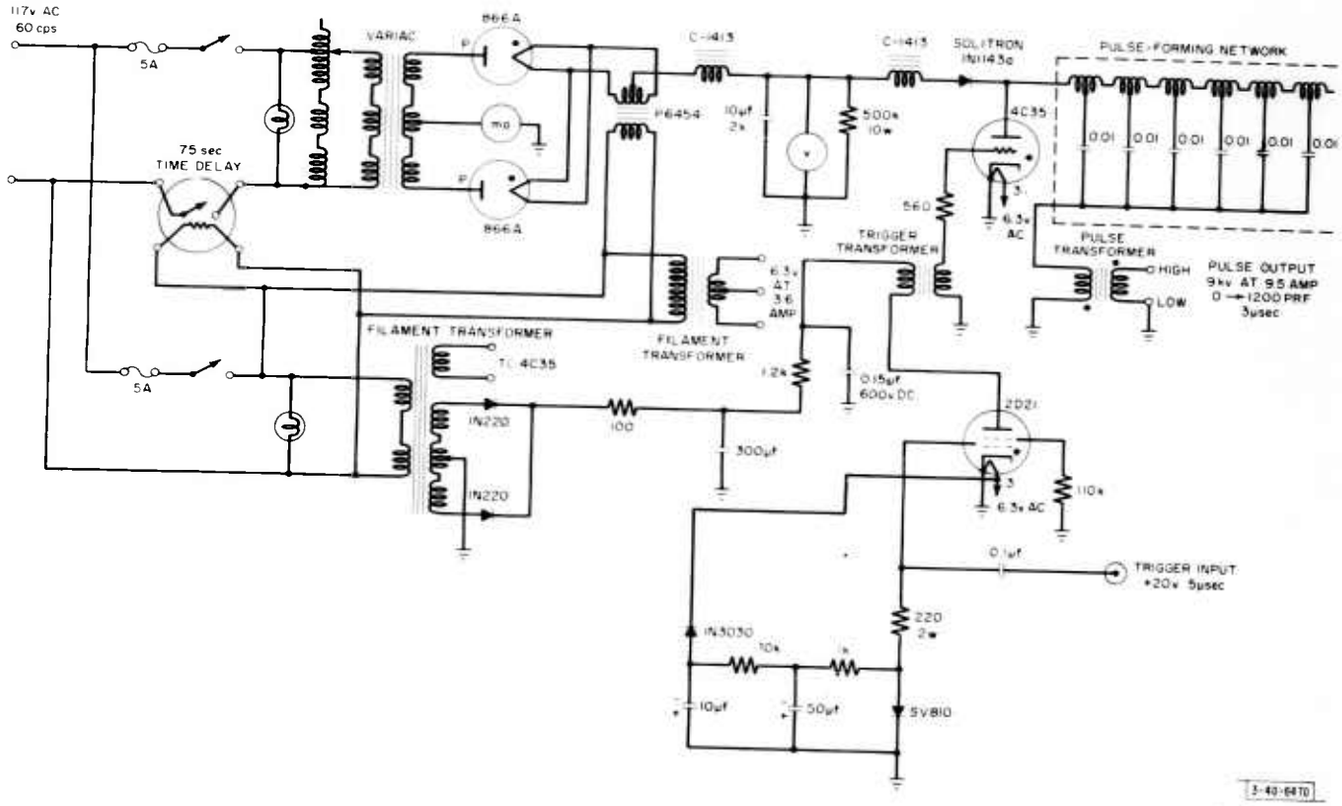

Fig. 30. Circuit diagram of Raytheon modulator for tetrode drivers.

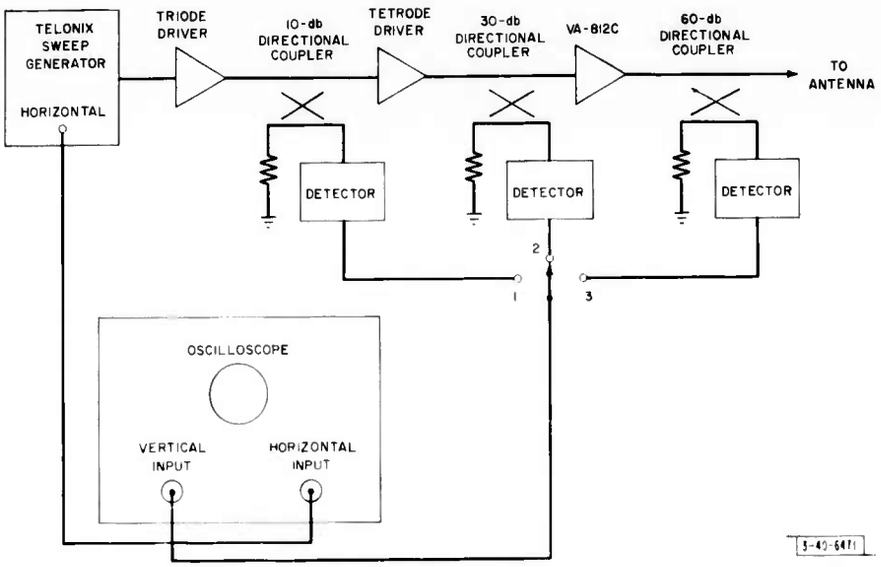

Fig. 31. Block diogrom far aligning transmitter.

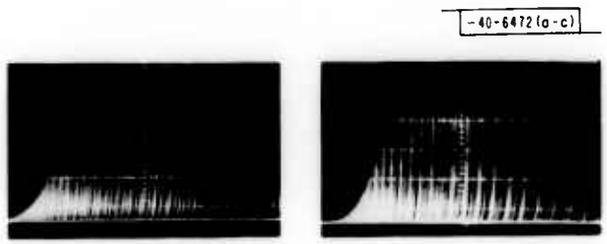

(o) Triade driver output. (b) Tetrode driver output.

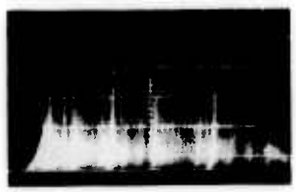

(c) VA-812C output.

Fig. 32. Possband of tronsmitter system. Center frequency, 420 Mcps. Horizantal scale, 5 Mcps/div.

The complete driver system was installed and checked out at the site. The performance characteristics were as given in Tables V, VI, and VII. At the present time, the equipment has been operating at the site for about one month with no serious malfunctions.

B. Final Amplifier and Modulator

1. Introduction

The modifications to the Wallops Island UHF final amplifier and modulator were completed in two phases. The first phase was directed toward increasing the repetition frequency capability from 320 to 960 pps. The second phase was concerned with broadbanding the final klystron amplifier of the transmitter chain.

The modulator used with this transmitter was designed to operate at pulse repetition frequencies up to 1200 pps with a 0.0033 maximum duty cycle. However, the performance of the modulator at 960 pps and a 0.0031 duty cycle was unreliable. Repeated DC overcurrent shutdowns occurred after 1 to 2 hours of operation at the normal 28-kv supply voltage. These shutdowns were traced to the thyratrons which occasionally failed to deionize after being pulsed.

Five trouble areas were uncovered within the modulator which contributed to this problem:

Network charging period,
Reservoir voltage metering,
Thyratron trigger circuitry,
Charging voltage unbalance across thyratrons,
Thyratron heating.

The corrective measures taken to alleviate the above discrepancies are discussed in Sec. III-B-3.

Broadbanding the final klystron amplifier was straightforward and presented no problem. Details of the broadbanding and klystron operating performance are discussed in Sec. III-B-6.

2. Description of Modulator

The modulator for the Wallops Island UHF transmitter is a Manson Laboratories Model 375. Detailed descriptions and circuit diagrams are given in Lincoln Laboratory Report 21G-011 [U] and Manson Laboratories "Instruction Manual for 27 Megawatt Modulator Model 375." The modulator is a standard line modulator, employing two General Electric Company Type 7390 hydrogen thyratron switch tubes in series. The pulse-forming network (PFN) is divided into two sections so that pulse lengths of 3.2 and 6.2 μsec may be obtained. For the short-pulse mode (0.2-μsec RF pulse duration) only the first section of the network is used to give a 3.2-μsec pulse on time for the modulator. The first section of the PFN contains twice as many capacitors (16) as the second section; full average power may be applied at the narrower pulse width. Operation at the short-pulse duration is accomplished by disconnecting the 1/2 inch copper tubing linking the first and second sections of the PFN. Figure 33 is a schematic diagram of the basic modulator as originally employed for the short-pulse, 960-pps mode.

3. Modulator Modifications

Network Charging Period:– The charging inductance (Fig. 33) consists of two 1.3-henry charging chokes in series. The second choke was installed to increase the network charging time, thereby increasing the reliability of thyratron deionization. At the 960-pps frequency, a problem arises due to this increased charging time. As stated earlier, the first

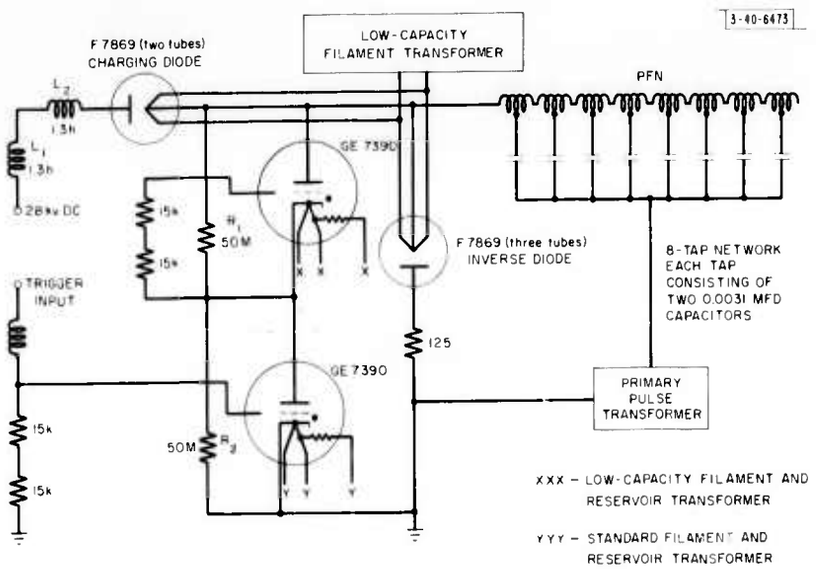

Fig. 33. Manson madulatar Model 375.

section of the PFN contains sixteen (31×10^{-10} farad) capacitors. The resonant charging period is 1130×10^{-6} sec. The pulse repetition period at 960 pps is 1040×10^{-6} sec. With the second choke in the circuit, the thyratrons were being pulsed at a rate faster than the resonant charging period. To correct this discrepancy, four capacitors were removed from the PFN to lower the resonant charging period to 975×10^{-6} sec. Removal of these capacitors also reduced the modulator voltage pulse width from 3.2 to 2.4 μsec as measured at the 70-percent voltage amplitude. However, this presented no problem at the short-pulse condition since the transmitted RF output pulse (0.2 μsec) was determined solely by the RF drive pulse to the final amplifier.

Reservoir Voltage Metering:– The reservoir voltages of the two hydrogen thyratron switch tubes were quite critical and judicious adjustments of these voltages were required at the 960-pps mode. This prohlem was further aggravated by the poor AC input line regulation at the site. To alleviate this latter situation, a General Radio Type 1570-AL automatic voltage regulator was installed to regulate both filament and reservoir voltages on the two thyratrons.

It was also discovered that the reservoir voltmeter for the upper thyratron, located on the control cabinet panel was reading approximately 0.5 volt (10 percent) too low. The panel meter was recalibrated against a standard voltmeter connected at the tube terminals. The calibration curve is plotted in Fig. 34.

Thyratron Trigger Circuitry:– As stated earlier the switching device in the modulator consists of two General Electric Company hydrogen thyratrons in series. Series arrangement of the tuhes was required to permit operation within the rated maximum peak voltage holdoff and anode dissipation factor. In the original version (Fig. 33), only the lower thyratron was triggered. When the lower tube fired, full network voltage (54 to 55 kv) was momentarily applied across the upper thyratron. Under these conditions, the rated peak voltage holdoff (33 kv) of the upper thyratron was exceeded by approximately 60 percent and the maximum anode dissipation factor was exceeded by 55 percent. This discrepancy was corrected by simultaneously triggering

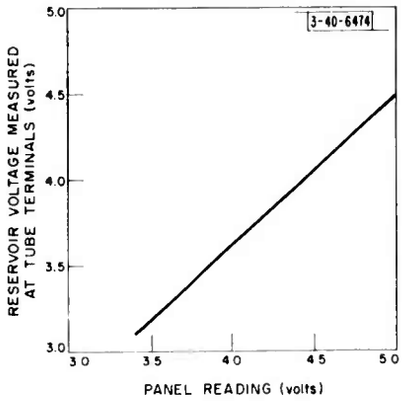

Fig. 34. Reservoir voltage vs panel meter reading for upper thyratron.

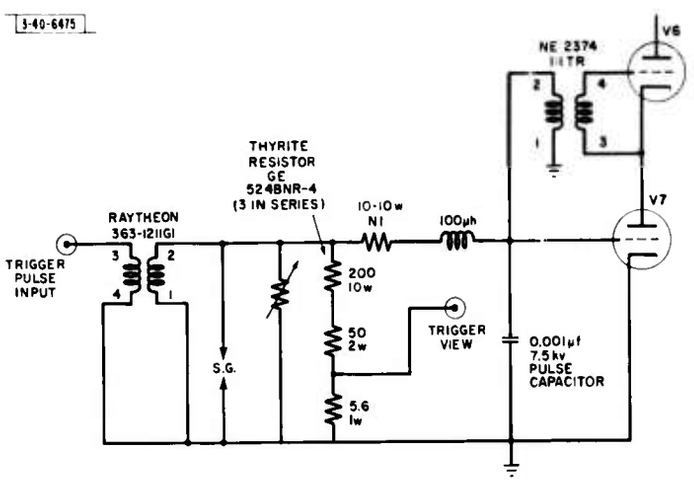

Fig. 35. Trigger input circuit for thyratrons.

both thyratrons. The modifications to the thyratron grid circuits which permitted individual triggers to be fed to each tube are shown in Fig. 35.

The original Manson trigger amplifier was found to be marginal in hoth output pulse amplitude and duration. This unit was replaced hy a 4C35 hydrogen thyratron amplifier (Fig. 36).

The loaded and unloaded trigger pulses at the grid of both tubes are shown in Fig. 37(a-c). Figure 37(a) is the loaded trigger pulse at the upper thyratron grid with no anode voltage applied. The loaded pulse at the lower grid is shown in Fig. 37(b), with no voltage applied. Figure 37(c) is the unloaded trigger pulsc.

Charging Voltage Unbalance Across Thyratrons:– The intended function of the resistance divider network R_1R_2 (Fig. 33) was to divide equally the charging voltage across the two thyratrons. We confirmed that the voltage distribution was determined primarily hy the ratio of the capacity across each tube and not by the resistors R_1 and R_2. The measured capacity across the top tube was 65 μμf and across the bottom tube 170 μμf. The charging voltage measured across the upper thyratron was approximately 1-1/2 times that across the lower tuhe. To distribute equally the voltage across both tubes, a 100-μμf capacitor in series with a 40-kohm resistor was shunted across the upper thyratron. The RC time constant was chosen to keep the capacitor from discharging its stored energy into the thyratron during the pulse.

The charging voltage waveforms are shown in Fig. 38(a-b) for 20-kv DC power supply voltage. Figure 38(a) corresponds to the voltage across the lower thyratron without the RC network

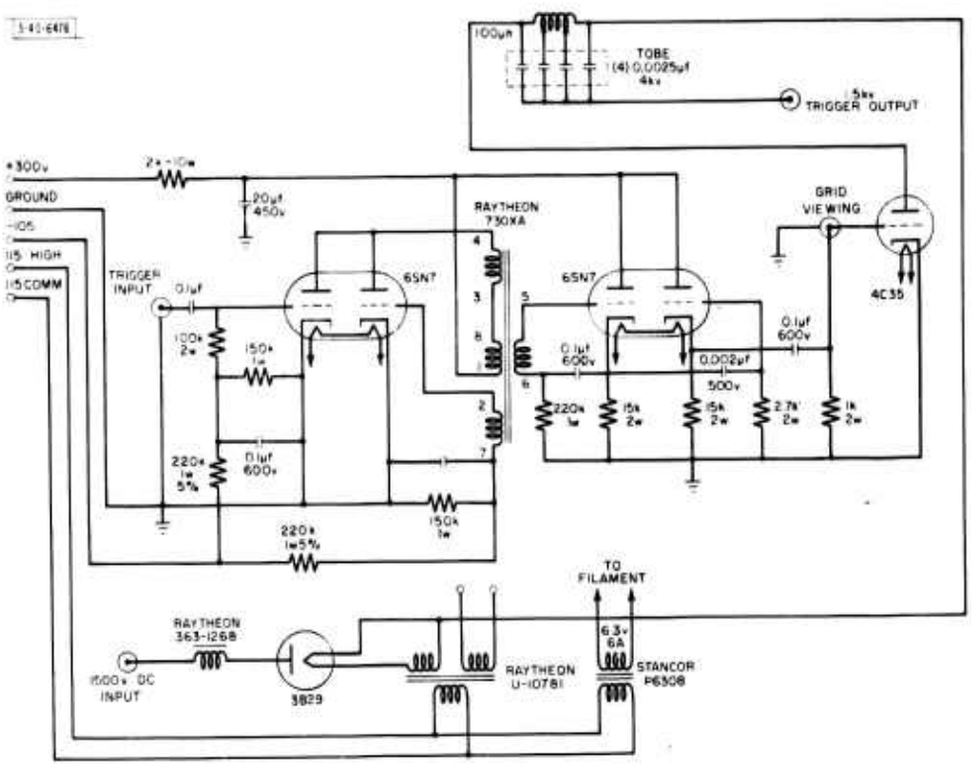

Fig. 36. Trigger amplifier. (NOTE: This drawing was taken fram Raythean Manufacturing Company, Power Tube Division, Drawing No. C100819.)

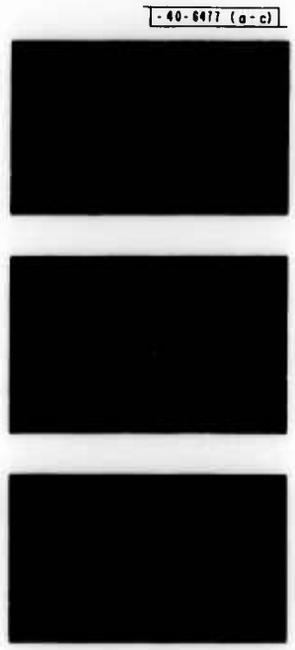

(a) Loaded pulse of upper thyratran.

(b) Loaded pulse af lower thyratran.

(c) Open circuit trigger pulse.

Fig. 37. Trigger pulses ot grids of both tubes. Horizantol time scale (right to left), 0.4 μsec/cm. Vertical sensitivity, 500 volts/cm.

(a) RC network nat cannected. (b) RC network connected.

Fig. 38. Chorging voltoge appearing across lower thyrotron and PFN. Horizontol time scale, 500 μsec/cm.

connected. Peak-to-peak voltage amplitude is 15.4 kv. In the figure, B is the 38.6-kv network voltage appearing across both thyratrons. We observe that the voltage (A) across the lower tube was still rising at the time the switch tubes were triggered, whereas the network voltage (B) had reached the peak of its charge cycle. With the RC network inserted, the voltage across the lower tube and the full network voltage are shown in Fig. 38(b), A and B, respectively. Peak-to-peak amplitude for the network voltage (B) was 38 kv. The voltage measured across the lower thyratron was 19 kv. The observed waveforms are identical.

Thyratron Heating:– Temperature measurements made before improvement of thyratron power division indicated that both thyratrons were running quite hot. The cathode-support temperature rise as a function of time is plotted in Fig. 39. It is interesting to note here that this heating was due only to the filament and reservoir power, since no anode voltage was applied during this test. Four fans were mounted on the modulator, directing air at the anode and grid of each tube. The following temperatures were recorded at 28-kv DC power supply voltage:

Upper anode 99°C	Upper grid 120°C
Lower anode 73°C	Lower grid 147°C

A 2-μh inductance was placed in series with the lower thyratron anode. This additional inductance provides an inverse voltage spike at the lower tube anode immediately after tube conduction ceases, thereby enhancing tube recovery. It is interesting to note that the energy stored in this inductance is approximately one joule as compared with the 0.08 joule stored in the 170-μμf capacity across the lower tube. This inductance is also in series with the distributed capacity shunted across the lower thyratron and so assists in keeping that capacitor from discharging its stored energy into the lower thyratron during the pulse.

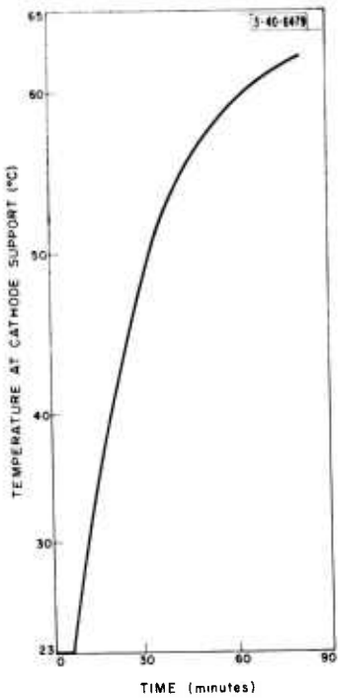

Fig. 39. Cathode-support temperature vs time.

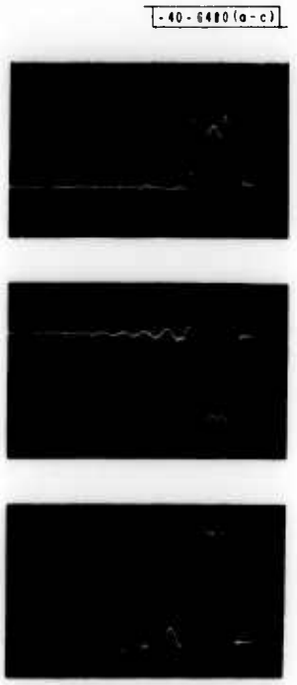

(a) Thyratron peak current pulse (555 amp/cm vertical sensitivity).

(b) Klystron peak current pulse (51.2 amp/cm vertical sensitivity).

(c) Klystran peak valtage pulse (40 kv/cm vertical sensitivity).

Fig. 40. Klystron peak valtage and current pulse. Horizontal time scale (right ta left), 2 μsec/cm.

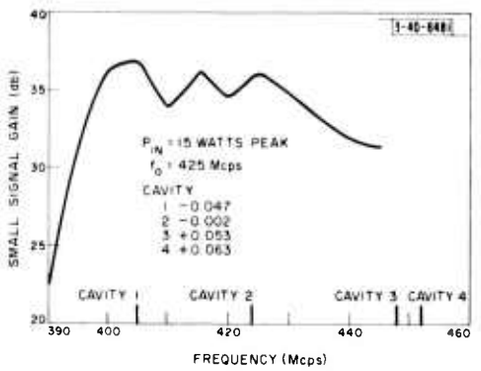

Fig. 41. VA-812C braad-band small signol gain.

4. Results

With the above-listed modifications incorporated into the system, the modulator has run continuously and reliably for repeated periods of 8 hours at 960 prf.

Tests were conducted at Annex II on a Manson modulator similar to the unit at Wallops Island. The results demonstrated the feasibility and reliability of operating the modulator for periods of 8 hours at 1200 pps, a 25 percent increase over the Wallops Island repetition frequency.

Tests were also conducted on a Kuthe thyratron Type KU274, a single tube replacement for the two GE 7390s. However, the thyratron was found to be defective and no further tests were scheduled.

5. Power Supply

The power supply for the Manson pulse modulator is an FXR-Z826A. This unit is described in detail in the Lincoln Laboratory Report 21G-0011 previously mentioned.

No modifications to the power supply were required.

6. Final Amplifier

The final amplifier in the transmitter chain is the Varian VA-812C waveguide output klystron amplifier. Operating characteristics for the VA-812C are described in the Varian Associates Final Report "UHF Klystron Transmitter (VA-812) Development Program," dated January 1961.

Figure 40(a-c) represents the klystron peak voltage and peak current obtained for a DC power supply voltage of 28 kv. The measured peak current in Fig. 40(b) is 148.5 amp. The peak voltage shown in Fig. 40(c) is 156 kv. The computed perveance is 2.4×10^{-6} amp/(volts)$^{3/2}$. Figure 40(a) is the thyratron peak current pulse, approximately 900 amp.

The tuning of the klystron was adjusted as follows for 425-Mcps center frequency:

Cavity	Frequency (Mcps)
1 (input)	405
2	425
3	444
4	452

The small signal gain obtained as a function of frequency is given in Fig. 41. These data were taken with constant input drive power of 15 watts peak.

The klystron was retuned for f_o = 432 Mcps with the cavity tuners set as:

Cavity	Frequency (Mcps)	Setting
1	412	58-1/2 half-turns CCW
2	431	44-1/2 half-turns CCW
3	455	26-1/2 half-turns CCW
4	459	13 half-turns CCW

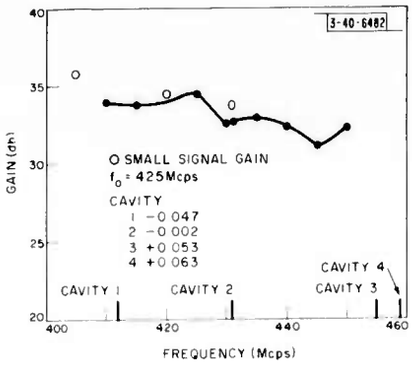

Fig. 42. VA-812C broad-band saturated signal gain.

(a) RF drive pulse to klystron.

(b) VA-812C RF output pulse.

Fig. 43. RF envelope, 1-μsec pulse durotion. Horizontal time scole, 0.4 μsec/cm. Horizontal sweep, right to left.

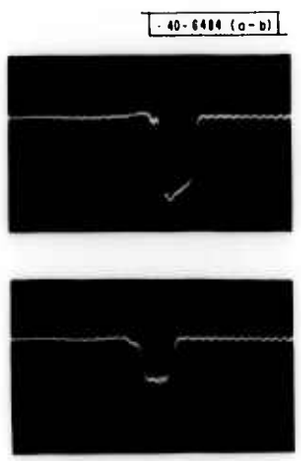

(a) RF drive pulse to klystron.

(b) VA-812C RF output pulse.

Fig. 44. RF envelope, 0.2-μsec pulse durotion. Horizontal time scale, 0.2 μsec/cm. Horizontal sweep, right to left.

The twelve klystron electromagnets were adjusted for maximum RF power output at the center frequency (432 Mcps). The magnet settings obtained were:

Magnet	Setting
1 (nearest cathode)	3.15A
2	3.55
3	6.9
4	3.8
5	4.9
6	4.6
7	5.4
8	3.7A
9	5.6A
10	4.6
11	5.7
12 (nearest collector)	4.0

The saturated signal gain obtained as a function of frequency is shown as the solid line in Fig. 42. The three circled points correspond to the small signal gain observed at 405, 420 and 432 Mcps, respectively. The saturated peak power output at 432 Mcps was 7.5×10^6 watts. Input peak drive power required was 3.8 kw. Measured beam efficiency was 32 percent.

The RF drive input pulse (432 Mcps) to the klystron is shown in Fig. 43(a), and the klystron RF output pulse in Fig. 43(b). Pulse duration is 1 μsec measured at the half-power points. The slight perturbation that appears near the leading edge of the klystron RF pulse was found to be insensitive to both the magnetic field and cavity tuning. The RF drive input pulse (0.2-μsec pulse duration) is shown in Fig. 44(a), and the corresponding klystron RF output pulse in Fig. 44(b).

C. Transmitter Synchronizer and Range Delay Unit

1. Transmitter Synchronizer

a. Introduction

The introduction of the high-repetition-rate, short-pulse mode of operation required that two changes be made in the system timing equipment: (1) introduction of additional circuitry for providing 960-pps synchronization and range tracking triggers to supplement the existing 320-pps triggers, and (2) substantial improvement of the time stability of these triggers relative to the 82-kcps crystal clock which is the basic source of all the radar timing. The first of these tasks could have been accomplished with relatively few additions to the timing system; however, a study of the circuitry used in the existing system indicated that the second of these tasks could not be accomplished without major revisions. Although the timing stability of the existing circuitry was good enough for use with the relatively long-pulse mode of operation, the short-pulse modification changed the stability requirements to something that could not be met without the use of high-speed logic. It was therefore decided that the majority of the timing equipment would be replaced by equipment of a new design.

The purpose of the transmitter synchronizer is to generate synchronous triggers at 960, 320 and 1280 pps, as well as 5120-cps square waves and a pretrigger occurring prior to each 320-pps pulse. The unit replaces the old trigger generator in the Wallops Island UHF radar.

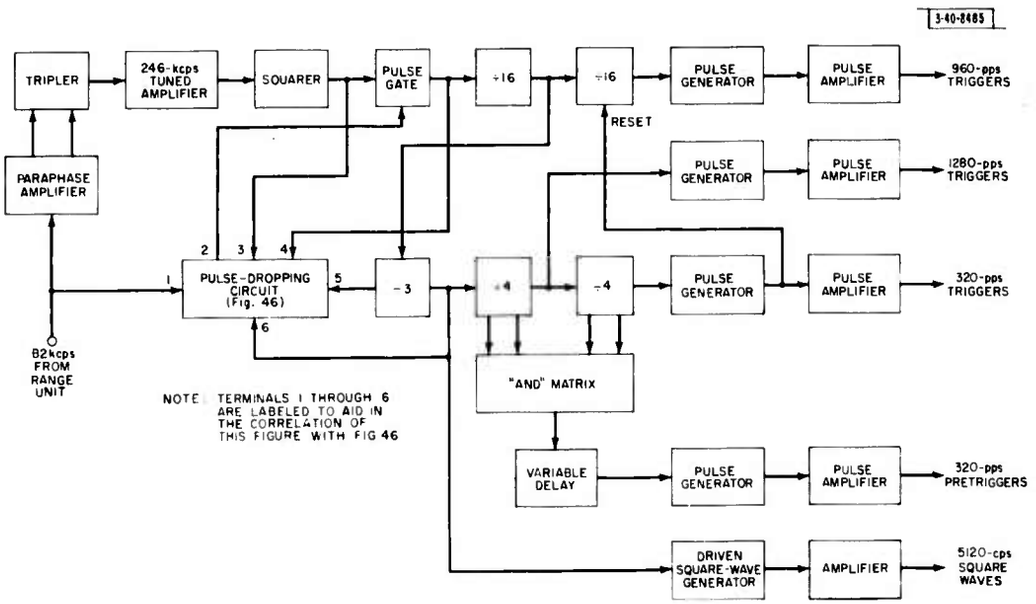

Fig. 45. Transmitter synchronizer.

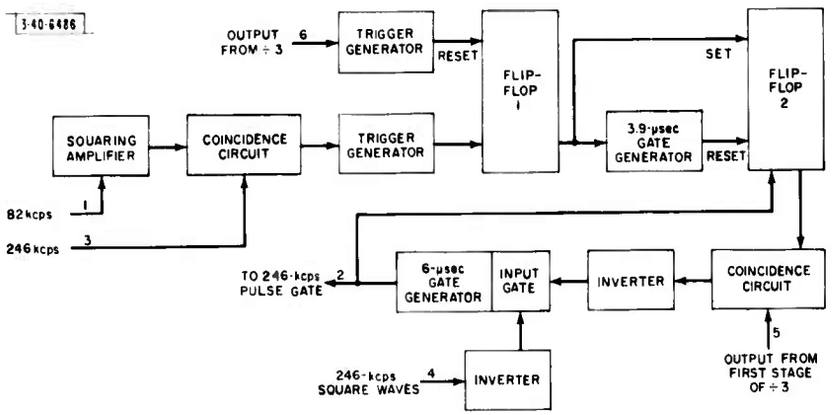

Fig. 46. Selective pulse-dropping circuit.

All triggers are 18 volts in amplitude at an impedance of 100 ohms and are 1 μsec wide. The 5120-cps square waves are 18 volts amplitude across 500 ohms. A selective pulse-dropping circuit is employed to insure a fixed-phase relationship between the triggers and the 82-kcps range clock. With the exception of the tripler circuits and the pulse amplifiers, the equipment was designed to use digital logic blocks supplied by Computer Control Company (hereafter called 3C). Figure 45 is a block diagram of the transmitter synchronizer.

b. Circuit Description

(1) Frequency Tripler:– An 82-kcps sine wave of 0.5-volt amplitude peak to peak is taken from the range clock and amplified by a paraphase amplifier. The two signals thus obtained are used to drive a push-pull frequency tripler followed by a tuned amplifier at a frequency of 246 kcps. This amplifier provides a sine wave of 5-volt amplitude peak to peak.

(2) 960-pps Triggers:– The 246-kcps sinusoid is squared by a 3C inverter and is then passed through a 3C gate used to selectively gate out pulses for phase-locking [see (7)]. The output of the gate is fed to a "divide by 16" circuit yielding 15360 cps, followed by a second "divide by 16" circuit yielding 960 cps. Each "divide by 16" circuit is a 3C, 4-bit binary divider (BC-30). The 960-cps square waves drive a pulse generator (DM-30) which generates 6-volt, 1-μsec pulses. An amplifier converts these to 18-volt pulses at an impedance of 100 ohms.

(3) 5120-cps Square Waves:– A "divide by 3" circuit (BC-30) is driven from the 15360-cps signal [see (2)] to produce a 5120-cps signal. The division is accomplished by use of a 2-bit binary divider with gated feedback, causing the output waveform to he a train of 130-μsec pulses at a repetition rate of 5120 pps. Square waves are generated by using these pulses as triggers for a 98-μsec one-shot multivibrator (DM-30). The signal is then amplified to a level of 18 volts peak to peak across 500 ohms.

(4) 1280-pps Triggers:– A "divide by 4" circuit (BC-30) is driven from the output of the "divide by 3" circuit [see (3)], yielding 1280 cps. This is followed by a pulse generator (DM-30) which produces 6-volt, 1-μsec pulses. An amplifier converts these to 18-volt pulses at an impedance of 100 ohms.

(5) 320-pps Triggers:– The 1280-cps square-wave signal (see above) drives another "divide by 4" circuit (BC-30) which produces 320-cps square waves. This is followed by a 1-μsec pulse generator (DM-30) and an amplifier whose output is 18-volt pulses at an impedance of 100 ohms. The output of the pulse generator also serves to reset the second "divide by 16" in the 960-pps trigger generating circuitry if necessary, thus insuring that the two will be synchronous when power is initially applied.

(6) 320-pps Pretriggers:– The assertion outputs of the last two "divide by 4" circuits [see (4) and (5)] are combined in an "and" configuration by use of 3C gates (DL-30) to produce a positive-going transient 196 μsec prior to each 320-pps trigger. This transient triggers a variable-delay multivihrator (DM-30) which, in turn, drives a pulse generator and pulse amplifier. The output is a 1-μsec pretrigger at an amplitude of 18 volts which may be positioned at any time from zero to 196 μsec prior to trigger generation.

(7) Selective Pulse-Dropping Circuit:– Figure 46 is a block diagram of the pulse-dropping circuit. The 82-kcps sine wave is passed through a squaring amplifier which is biased

to produce negative pulses of approximately 4-μsec duration at an 82-kcps repetition rate. These pulses are used to enable a gate (DI-30) which is fed with 246-kcps square waves. The output of this coincidence circuit is a train of 4-μsec pulses at a repetition rate of 82 kcps which bears a fixed-phase relationship to the 82-kcps range clock output. A trigger generator (DM-30) is driven by this train and the output is used to set flip-flop 1 (FF-30). This flip-flop is reset by a pulse generated from the output of the "divide by 3" circuit. When power is initially applied, the state of all binary dividers is unknown, with the result that the output of the "divide by 3" circuit may bear any one of three discrete phase relationships to the 82-kcps clock. This condition is manifested in the output of flip-flop 1 which is a pulse of width n, n+4, n+8 μsec, where n is some small time less than 4 μsec and is dependent upon the various circuit delays in the system. This pulse is used to set flip-flop 2, as well as to trigger a 3.9-μsec pulse generator for resetting flip-flop 2. This type of circuit (FF-30) is a "DC" flip-flop in that when positive logic is applied to both set and reset terminals, the input which is removed last determines the state of the output. Thus, if the output of flip-flop 1 is either n+4 or n+8 μsec in duration, flip-flop 2 will settle in a "set" state. Conversely, if the output of flip-flop 1 is n μsec (less than 3.9 μsec), flip-flop 2 will become reset.

The negative portion of the output waveform from the first stage of the "divide by 3" circuit occurs about 65 μsec after the final state of flip-flop 2 has been determined. These two signals are fed to a coincidence circuit (DI-30) whose output is inverted (DI-30) and applied as an enable circuit for a 6-μsec gate generator (DM-30). If the output of flip-flop 1 is either n+4 or n+8 μsec in duration, this gate generator is enahled 65 μsec later. If it is n μsec in duration, there is no enabling signal. The first 246-kcps pulse (inverted) that appears after the arrival of the enabling gate triggers the pulse generator, causing a 6-μsec inhibit pulse to be applied to the 246-kcps pulse gate described in (2). The result is that one pulse of the 246-kcps train is prevented from triggering the chain of dividers. The output of the 6-μsec pulse generator is also fed back to immediately reset flip-flop 2, thus preventing the elimination of more than one count at a time. When one count is dropped, the waveform from flip-flop 1 decreases in length by 4 μsec. The width of this pulse is examined 5120 times per second by flip-flop 2 to determine whether or not one count should be dropped. Pulse inhibition may he required up to two times in order that the output of flip-flop 1 be degenerated to less than 4 μsec, after which time no more counts are dropped.

This selective pulse-dropping circuit will always force the triggers into a set phase relationship to the 82-kcps clock within 400 μsec after the application of supply voltage.

2. Range Delay Unit

a. Introduction

The purpose of the range delay unit is to generate triggers at 960 and 320 pps which are synchronous with the n^2 gate of the old SCR-584 radar range unit. The unit replaces the old range delay generator in the Wallops Island UHF radar. These triggers are 18 volts in amplitude at an impedance of 100 ohms, and are 1 μsec wide. A conditional synchronizing circuit provides for resetting all the dividers should a trigger fail to coincide with the n^2 gate. As with the transmitter synchronizer, the range delay unit was designed to use digital packages manufactured by Computer Control Company. Figure 47 is a block diagram of the range delay unit.

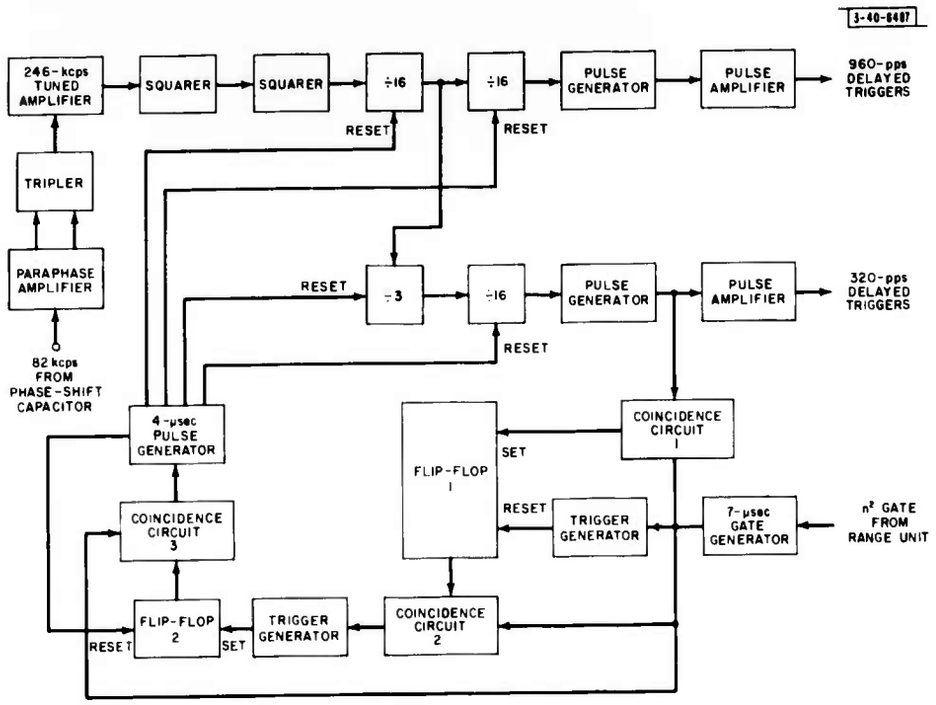

Fig. 47. Range delay generator.

h. Circuit Description

(1) Frequency Tripler:– The circuit is identical to the frequency tripler used in the transmitter synchronizer and is interchangeable with it. The input is an 82-kcps sinusoid taken from the output of a mechanical phase-shift capacitor, and the output is a 246-kcps sinusoid with an amplitude of 5 volts peak to peak.

(2) 960-pps Delayed Triggers:– The chain of circuits which generate the 960-pps delayed triggers differs in two respects from the circuits which produce the 960-pps triggers in the transmitter synchronizer. The second squarer, although it is the same circuit (DI-30) as the pulse gate in the synchronizer, is permanently enabled. Hence its sole function is the amplification and shaping of the 246-kcps signal. The other difference from the transmitter synchronizer is that all dividers may be reset by the synchronizing circuit described in (4). The delayed triggers are 18 volts in amplitude at an impedance of 100 ohms with the amount of delay determined by the position of the n^2 gate.

(3) 320-pps Delayed Triggers:– The chain of circuits which generates the 320-pps delayed triggers is similar to that in the transmitter synchronizer, the only difference is that the dividers may be reset when the 960-pps delayed triggers are reset. The synchronizing line from the 320-pps triggers to the 960-pps triggers is omitted in this unit, since all reset lines are pulsed simultaneously from a separate circuit. The output is 18-volt, 1-μsec pulses at an impedance of 100 ohms.

(4) Conditional Synchronizing Circuit:– The conditional synchronizing circuit guarantees that the delayed triggers occur simultaneously with the n^2 gate. At gate time a small interval of time (7 μsec) is examined by flip-flop 1 for the presence of a trigger; and if one occurs, no further action is taken. If no trigger has appeared by the termination of the interval, a sequence of events is initiated to generate a synchronizing pulse at the time of the next n^2 gate.

A 7-μsec pulse generator (DM-30) is triggered by the n^2 gate and the output is fed to three coincidence circuits (DI-30) and a trigger generator (DM-30). The leading edge of the gate causes flip-flop 1 to be reset, producing a "go" condition at coincidence circuit 2. The other input to this circuit is enabled at the trailing edge of the 7-μsec gate and a trigger is generated to set flip-flop 2. This produces a "go" condition at coincidence circuit 3, which will now have an output at the time of the next n^2 gate. This output triggers a 4-μsec pulse generator which produces a pulse to synchronize all dividers with the n^2 gate. The pulse is also fed back to immediately reset flip-flop 2, thus preventing the generation of more than one pulse. Should the dividers already be synchronized to the n^2 gate, a 320-pps trigger will be generated during the 7-μsec gate, producing an output from coincidence circuit 1. This pulse sets flip-flop 1, causing a "no go" condition at coincidence circuit 2 when the trailing edge of the 7-μsec gate arrives. Therefore, flip-flop 2 remains reset, there is a "no go" condition at coincidence circuit 3, and no 4-μsec pulse is generated.

The conditional synchronizing circuit assures that the delayed triggers are coincident with the n^2 gate within 7 msec after the application of supply voltage.

D. Frequency Synthesizer

With the changeover of the Wallops Island UHF radar to short-pulse operation, it beeame desirable to provide coherent oscillators for the receiving system rather than to continue the use of a laboratory signal generator for a local oscillator. In addition, the wider bandwidths associated with the short pulses made a shift of the IF frequency from 30 to 60 Mcps desirable.

The Special Radars Group (41) undertook the design and construction of the new frequency synthesizer. Figure 48 is a block diagram of the unit, which generates eoherent exciter, stalo and coho frequencies.

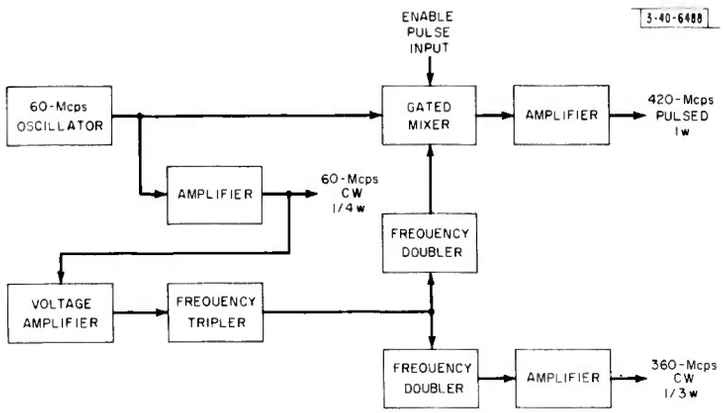

Fig. 48. Frequency synthesizer.

The equipment operates as follows: A 60-Mcps signal is generated by a crystal-controlled oscillator and is passed through a power amplifier. The amplifier delivers 250 mw of power for use as a coho signal in the phase-detecting equipment. This signal is also passed through a chain consisting of a voltage amplifier and a frequency tripler. The 180-Mcps waveform thus generated is then passed successively through a frequency doubler and a power amplifier. This amplifier puts out 300 mw of power at 360 Mcps for use as a stalo frequency in the receivers. The 180-Mcps waveform is also fed through a separate frequency doubler and thence to a gated mixer where it is combined with the original 60-Mcps signal and gated by a 10-μsec externally applied pulse. The resulting pulse of 420-Mcps energy is amplified by a power amplifier to a level of 1 watt of peak power for use as the transmitter exciter signal. All three outputs are at an impedance of 50 ohms.

IV. RECEIVER

A. Introduction

The receiver described in this section is the equipment which links the front-end mixer-preamplifier with the display and recording equipment. The section is divided into three parts: one for each separate chassis of the receiver.

The multiplex and quadrature-video chassis converts the 60-Mcps receiver IF to two quadrature-video components in real time, and with sufficient gain to provide 40 db of dynamic range from amplified front-end noise to output saturation. A second channel provides a time-delayed, reduced-gain version of the IF, which is multiplexed with the real-time channel to yield an over-all split dynamic range of 80 db.

The multiplex-timing and sample-and-hold chassis provides the control signals which gate the high- and low-gain channels in the multiplex and quadrature-video chassis. In addition, a sample-and-hold circuit is connected to each quadrature-video output. The sample-and-hold circuits permit acquisition by DATRAC (analog-to-digital converters by Epsco, Inc.) of one 50-nsec sample of each quadrature-video component per pulse repetition interval.

The test-pulse generator chassis produces a 60-Mcps, 0.07-μsec pulse, which can be used to set the delays in the sample-and-hold chassis to conform with the multiplexing time delay. The generator chassis is also useful for checking over-all operation of the receiver.

B. Multiplex and Quadrature-Video Chassis

1. Operation

Figure 49 is a simplified block diagram which shows the relationship of the multiplex and quadrature-video chassis to the rest of the receiver. The 60-Mcps IF input is split into two channels, one of which is delayed in time and has less gain than the other. The two channels are time multiplexed into a pair of phase detectors which resolve the IF into its quadrature-video components. The quadrature-video outputs are routed to the sample-and-hold circuits and also to the oscilloscopes used for photographic recording.

The time relationship of signals at various points in Fig. 49 is shown in the timing diagram of Fig. 50. The time reference is the leading edge of return pretrigger from the range tracker. This precedes the actual return by approximately 6 μsec. Both IF channels are shut off for one microsecond following the pretrigger to establish a zero-signal (noise-free) reference for the quadrature-video outputs. The high-gain channel is turned on for roughly 59 μsec, after which

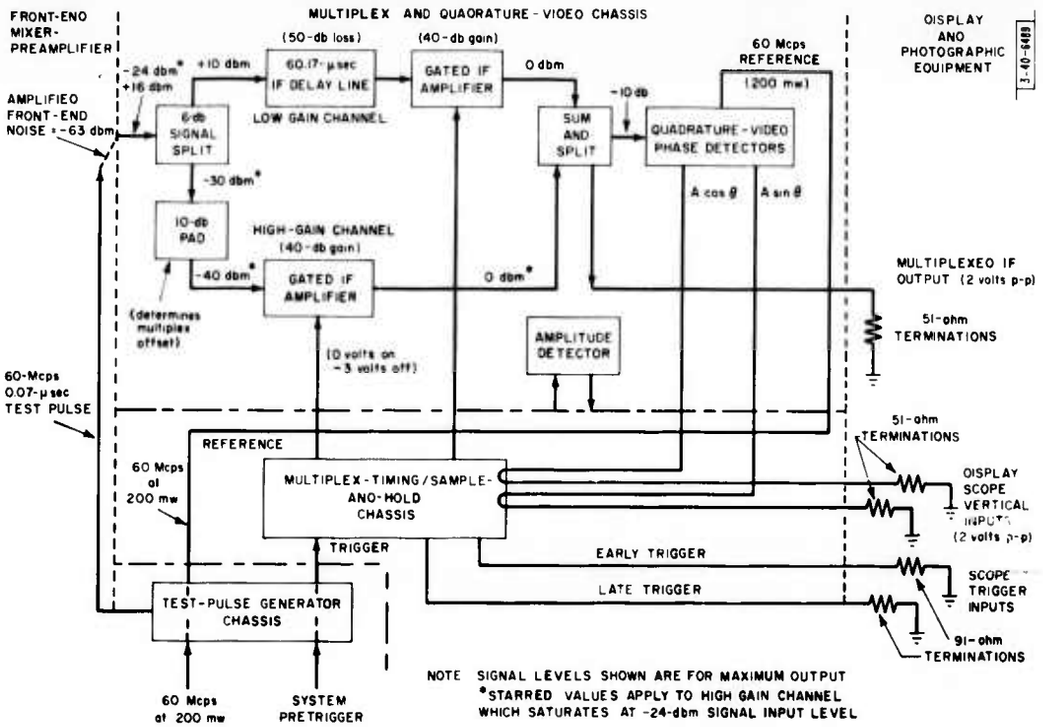

Fig. 49. Multiplex and quadrature-video chassis relationship to rest of receiver.

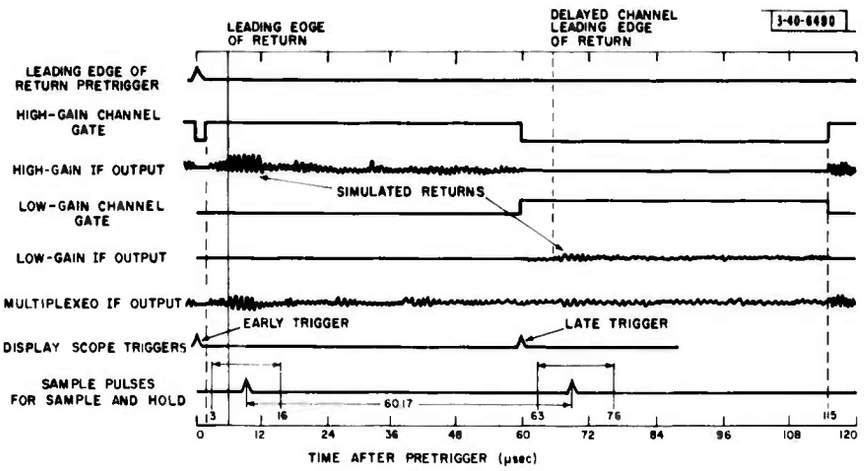

Fig. 50. Time relatianship of signals at various points in Fig. 49.

the (delayed) low-gain channel is turned on for 55 μsec. Then the high-gain channel is turned back on and remains on until the next pretrigger.

The system design is based on an assumed receiver noise level at the IF input of −63 dbm (receiver noise temperature = 100°K, bandwidth = 40 Mcps, 40-db gain). The high-gain channel is set up to handle the first 40 dh of input dynamic range, and the low-gain channel accommodates the top 40 db. The output level is a 1-volt peak (2 volts peak to peak) into 50 ohms for maximum signal input.

A multiplexed IF output is available at the front panel with a 2-volt peak-to-peak maximum output into 50 ohms. This IF output can be used directly or it can be connected to the internal-amplitude detector, which has good rise time but poor linearity and dynamic range. An external amplifier can be inserted between the multiplexed IF output and the amplitude-detector input to increase the sensitivity, if desired.

2. General Description

Figure 51 is a block diagram of the multiplex and quadrature-video chassis, showing the individual units that make up the chassis. Photographs of the finished chassis are shown in Fig. 52. The top view shows the heat sink for the 60.17-μsec quartz delay line in the upper-left corner and the two phase detectors and one amplitude detector on the right. The power supplies are located next to the front panel. The bottom view shows the gated IF amplifiers and other smaller components.

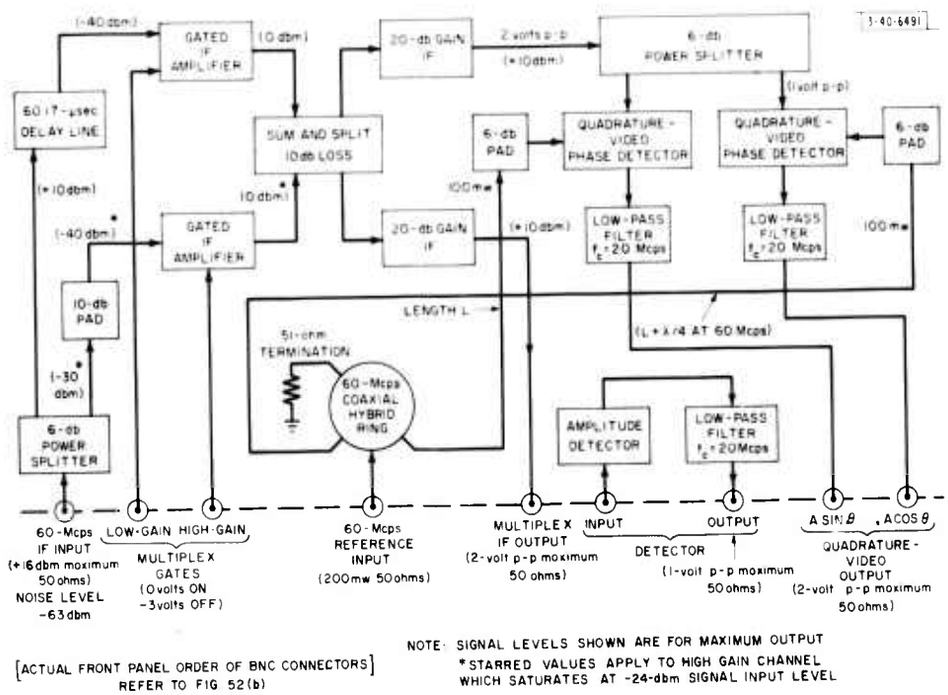

Fig. 51. Multiplex and quadrature-videa chassis.

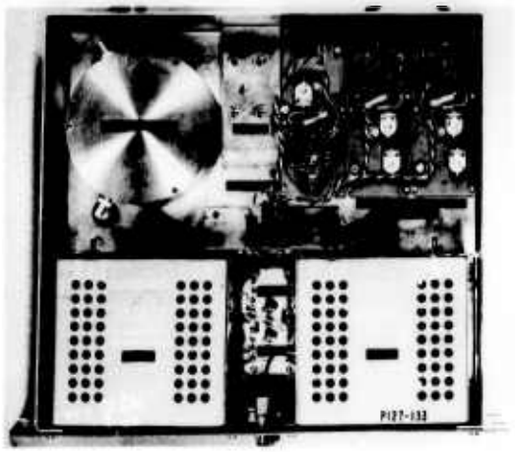

(a)

(b)

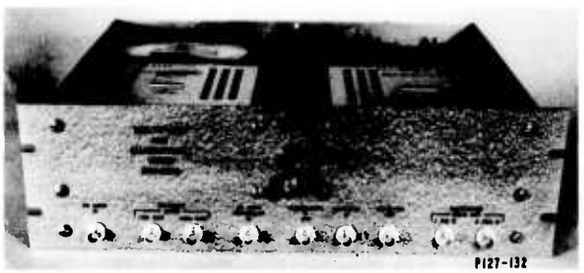

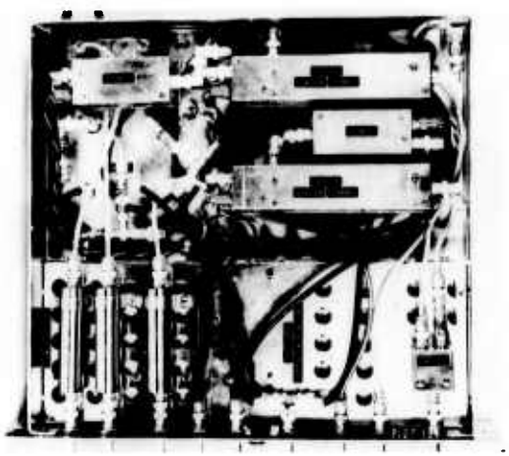

(c)

Fig. 52. Multiplex and quadrature-video chassis, showing top, front and bottom.

3. Design Objectives

The design objectives were:

Output-pulse rise time better than 35 nsec,

Single-channel dynamic range of 50 db,

Better than 40-db isolation between phase detectors,

Better than 80-db channel-on/channel-off ratio,

Multiplex switching time of 0.5 μsec,

Little pulse-shape distortion,

Symmetrical plus-and-minus voltage outputs for equal plus-and-minus phase angles (2-volts peak to peak into 50 ohms at maximum signal),

Miminum phase transients near 0° and 180°.

4. Actual Performance

Most of the design objectives were met without qualification. There is a small amount of pulse-shape distortion, which is primarily due to a compromise between loss and impedance match in the signal splitters and combiners. Better performance could be obtained with directional couplers, but the size would be much greater.

The phase-detector output exhibits some asymmetry at maximum signal level. This asymmetry is a function of the 60-Mcps reference level (and diode match). Photographs of measured performance and a description of the components are presented in Sec. IV-B-5.

5. Gated IF Amplifiers

The gated IF amplifier of Fig. 53 is an adaptation of a wide-band transistor IF amplifier design developed by J. DiBartolo of Group 41. Transformers were selected to provide 40 Mcps of bandwidth (Fig. 54) centered at 60 Mcps. A gate circuit was added to switch off the emitter current of the first three stages in response to a −3-volt gate-signal input. The circuit is arranged so that the IF amplifier is on when no gate signal is applied, in order that it may be used as a conventional IF amplifier, if desired. The gating characteristics are shown in Fig. 55. The amplifier switches from transmission to 80 db of rejection in 0.5 μsec, and vice versa. A deliberate delay of a few tenths of microsecond is introduced in turn-on so that two IFs can be gated with complementary waveforms without both amplifiers ever being on together. (The turn-on delay compensates for the finite turn-off time.) The amplifier gain is 40 db and it can supply 2 volts peak to peak into 50 ohms.

6. 20-db Gain IF

The 20-db gain IF amplifier is used as a buffer amplifier level booster, and has essentially the same performance as the gated IF amplifier described above, except that it is ungated and the gain is lower. A photograph of the amplifier is shown in Fig. 53 (small unit).

7. 60-Mcps IF Delay Line (Quartz)

The 60-Mcps IF delay line is a commercial unit which has been enclosed in a brass heat sink to reduce the short-term delay vs temperature variations. Without the heat sink, the delay was observed to change by one-half a cycle of the 60-Mcps IF (8 nsec) in a period of a few minutes. The heat sink improves matters, but if true phase coherence between the high and low channels were desired, an oven would be a necessity.

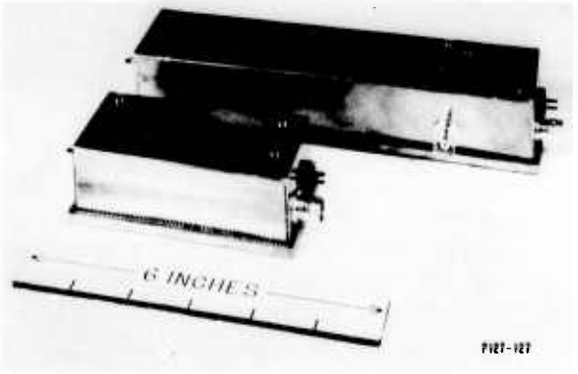

Fig. 53. Gated IF amplifier (lang unit) and 20-db gain IF (shart unit).

Fig. 54. Frequency response of gated IF amplifier. The morkers are at 40 ond 80 Mcps. The response with 3-db additional attenuatian is superimposed.

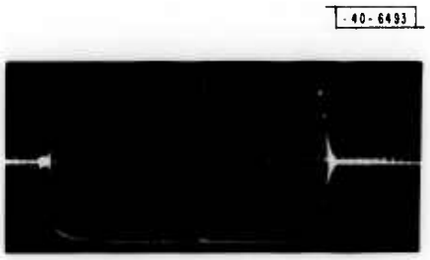

Fig. 55. Goting characteristics af gated IF omplifier. Harizontal scole, 0.5 μsec/cm; vertical scole, −0.5 valt/cm (into a 50-ahm load). Carrier frequency, 50 Mcps.

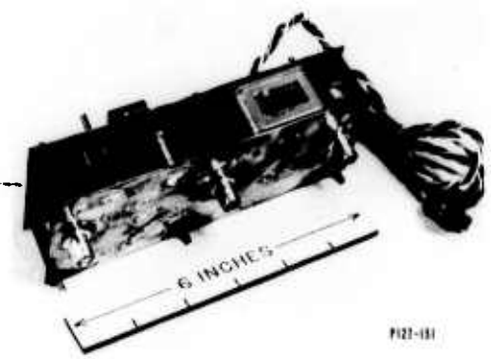

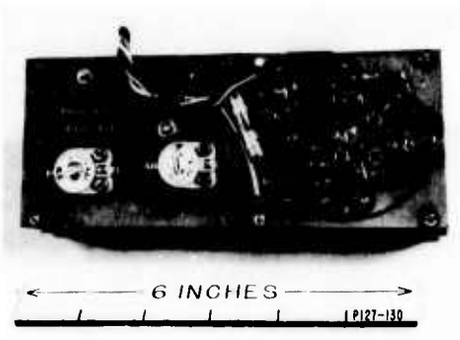

Fig. 56(a-b). Quadrature-videa phase detector. (a) Side view. (b) Tap view showing wide-band videa amplifier. The adjustments, fram left to right, are: phase trim, 60-Mcps trap, DC zera odjust, ond gain trim.

The delay line was obtained on a short time schedule and was not quite as ordered, but was found to be acceptable. This accounts for the 60.17-μsec delay (55 μsec was ordered) and the 100-ohm impedance level (used in a 50-ohm system). The delay line specifications are as follows:

Delay	60.17 μsec
Center frequency	60 Mcps
Bandwidth	> 25 Mcps
Spurious	< −50 db
Attenuation	48 db (100-ohm source and load)

8. Power Splitters

A 60-Mcps coaxial hybrid ring (constructed of 73-ohm cable to provide 50-ohm port impedances) is used to split the 60-Mcps reference signal for the two quadrature-video phase detectors. The hybrid provides about 28-db isolation with minimum loss. A 6-db pad in front of each phase detector brings the total isolation between phase detectors to better than 40 db.

Signal splitting and combining are accomplished in resistive devices to accommodate the wide-signal bandwidth. A compromise is made between loss and impedance match. (The match would be good, if all other components presented good matches to the splitters.) There are three 6-db splitters (one commercial unit), and one sum-and-split unit which sums two inputs and provides two outputs. The loss from one input to one output is 10 db.

9. Quadrature-Video Phase Detectors

One of the quadrature-video phase detectors is shown in Fig. 56. The phase detector itself consists essentially of a wide-band transformer and two diodes. The rest of the unit is a wide-band video amplifier capable of more than a 2-volt peak-to-peak output into a 50-ohm load. The video-amplifier frequency response is 40 cps to 30 Mcps. The video amplifier is DC coupled out to avoid the need for a very large coupling capacitor. (A DC zero adjust is provided to set the DC output level to zero.) The video amplifier must have a 50-ohm output impedance in order to properly drive the low-pass filter which follows it. (The low-pass filter has the desired video-pulse response only when driven from and terminated in 50 ohms.) Figure 57(a-d) shows the output of the phase detector (plus low-pass filter) for four different signal-phase conditions (relative to the 60-Mcps reference). The 250-nsec signal input pulse is shown in Fig. 57(e). The vertical sensitivity is increased by ten times for the 0° and 180° phase conditions. The phase transients are seen to be about 0.1 of the 90° ($\sin\theta = 1$) amplitude and thus correspond to 0.1 radian or about 6° peak-phase error. The phase-detector schematic is shown in Fig. 58.

10. Amplitude Detector

A small modification of the phase-detector circuit changes it to an amplitude detector with the same general output characteristics (rise time 35 nsec) but unipolar output. The modification consists of reversing one of the diodes so that they form a full-wave rectifier for the 60-Mcps signal pulse. The 60-Mcps reference input is not needed but in its place a 7.5-ma bias current is used to increase the detector's sensitivity to small signals. This bias current can be supplied internally by connecting the reference input to +10 volts through a 1.2-kohm resistor.

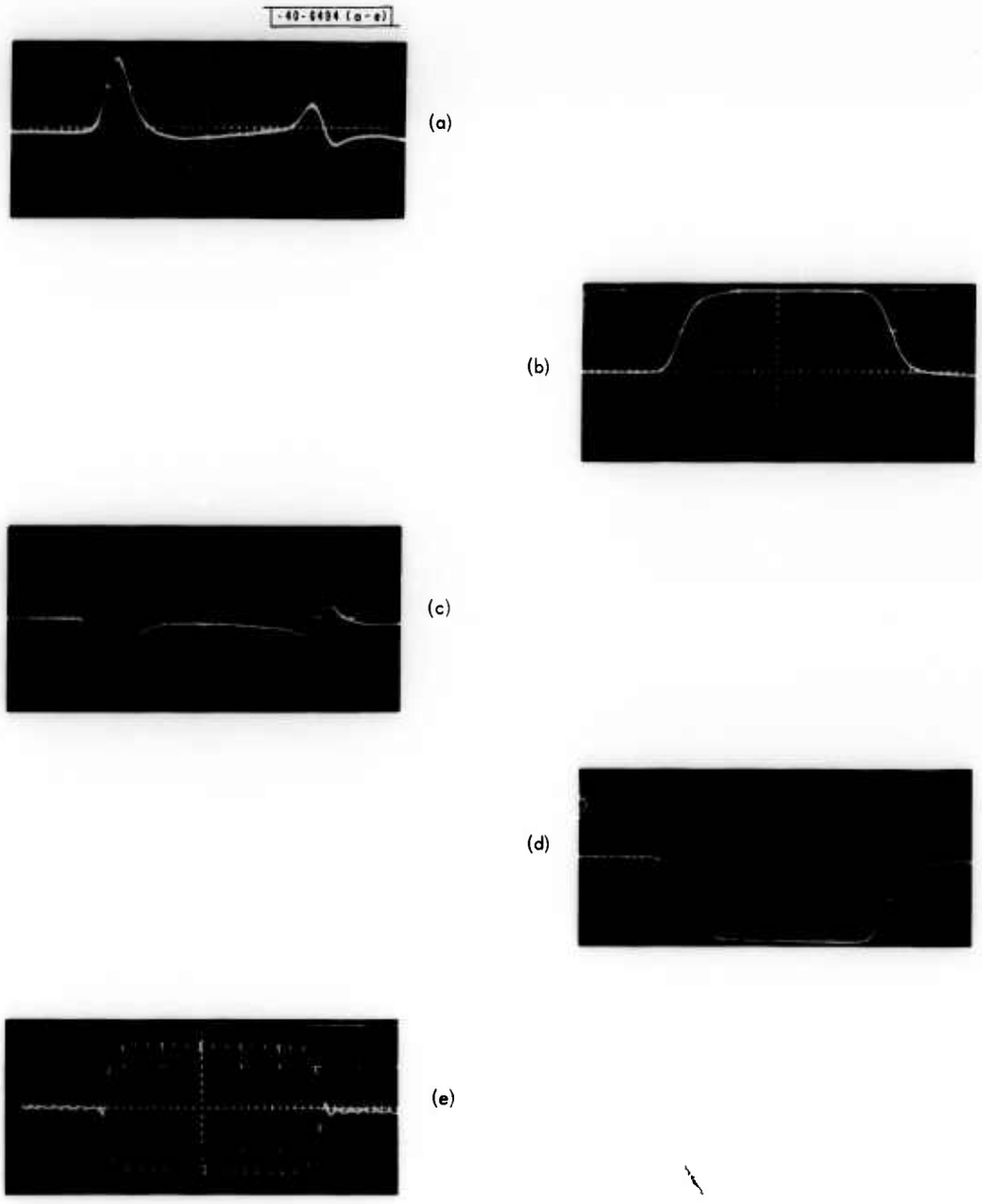

Fig. 57. Phase detectar autputs vs signal phase θ at 0°, 90°, 180°, and 270°. Horizantal scale, 50 nsec/cm; vertical scale, 0.5 volt/cm for 90° and 270°, and 0.05 valt/cm far 0° and 180°. The input pulse of 60 Mcps is shown in (e).

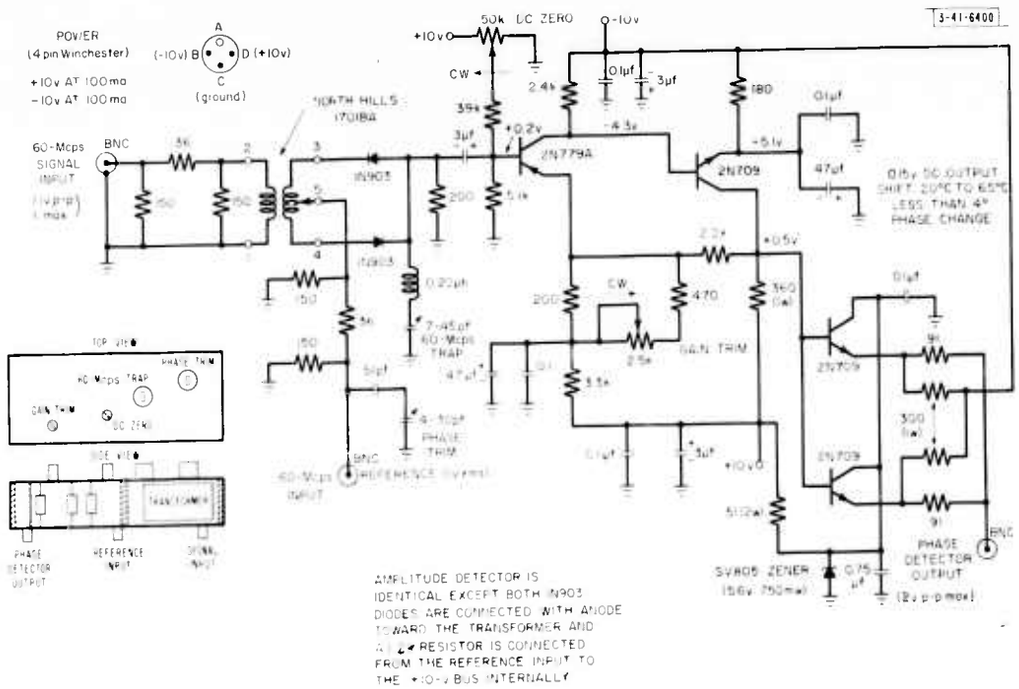

Fig. 58. Quadrature-video phase detector schematic.

The output waveform for maximum-pulsed signal input is shown in Fig. 59. The amplitude detector is not very linear and has limited dynamic range (about 30 db), but this range is the best that could be achieved (with good rise time) given the low signal levels available from the transistor IF amplifiers (2-volt peak-to-peak maximum).

11. Low-Pass Filter

Both the phase and amplitude detectors require an external low-pass filter to remove vestigial 60-Mcps components which remain despite the action of the 60-Mcps trap circuit. This filter should provide at least 40 db of attenuation at 60 Mcps and still affect the output pulse shape and rise time as little as possible.

The low-pass filter is a modified 7-pole Butterworth filter designed to be driven from 50 ohms and terminated in 50 ohms. The modification of the filter consists of a 100-ohm resistor paralleled with the center inductor, which essentially reduces the filter overshoot to zero. The nominal 3-db cutoff frequency is 20 Mcps and the rise time is about 25 nsec. Figure 60 shows 100-nsec input and output pulses superimposed except for a small vertical offset.

The filter was built in a coaxial structure to provide a solid-ground path and the resulting package is shown in Fig. 61. The filter design can be readily scaled to provide other video bandwidths.

C. Multiplex Timing and Sample-and-Hold Circuits

Two DATRACS will be used to quantize the quadrature video: one for A sin Θ, and one for A cos Θ. To make an analog-to-digital conversion, the DATRACS require an input which is held

Fig. 59. Amplitude detectar autput wavefarm with maximum pulse signal input (2 valts peak ta peak). Harizantal scale, 50 nsec/cm; vertical scale, 0.5 valt/cm.

Fig. 60. Pulse respanse af law-pass filter. The 100-nsec input and autput pulses are shawn superimposed. The lawer trace is the input pulse; the upper trace, the autput pulse. Harizantal scale is 50 nsec/cm.

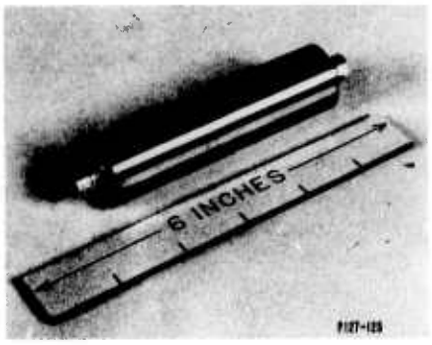

Fig. 61. Law-pass filter.

constant for about 40 μsec. Therefore, a sample-and-hold circuit (boxcar) is used before each DATRAC to sample the video at a known time (the leading edge of the target, or some fixed time later) and to hold the sampled voltage for 40 μsec or longer. The aperture of the boxcar (less than 50 nsec) is chosen so that it is consistent with the video bandwidth of 10 Mcps. An input amplifier for each boxcar (Fig. 62) is AC coupled and has a 3-db bandwidth from 5 cps to 17 Mcps. The output amplifier is DC coupled and has a rise time of less than 0.5 μsec into 500 pf (the approximate capacitance of the unterminated coaxial cable to the DATRAC input). The linearity of the boxcar and amplifiers has been measured at ±1 percent and the storage error is 1 percent or less over a 60-μsec period.

Each quadrature-video signal, as described in Sec. IV-B-1, consists of two time-multiplexed parts; the first comes from a high-gain channel, the second, 60.17 μsec later, comes from a low-gain channel. Each boxcar, therefore, must perform two sample-and-hold operations, 60.17 μsec apart, every radar period. The timing circuits are triggered by a pulse (system pretrigger) which precedes the target leading edge by a precisely known amount of time, approximately 6 μsec. To sample the leading edge of the target, the 3- to 16-μsec variable delay should be set at 6 μsec. The 60.17-μsec delay must exactly equal the IF multiplexing delay. These delays can be set by a test pulse generator which will be described in Sec. IV-D.

The delays are generated by monostable multivibrators, which are compensated to minimize changes in delay due to variations in ambient temperature. Silicon transistors were chosen to eliminate the temperature dependence of I_{cbo}. The remaining factors contributing to thermal instability of delay are: the thermal coefficients of the timing capacitor and resistor, temperature-dependent voltage drops across emitter-base and diode junctions (which decrease about 2 mv/°C), and Zener diode temperature coefficients. The method used to stabilize the delay is determined

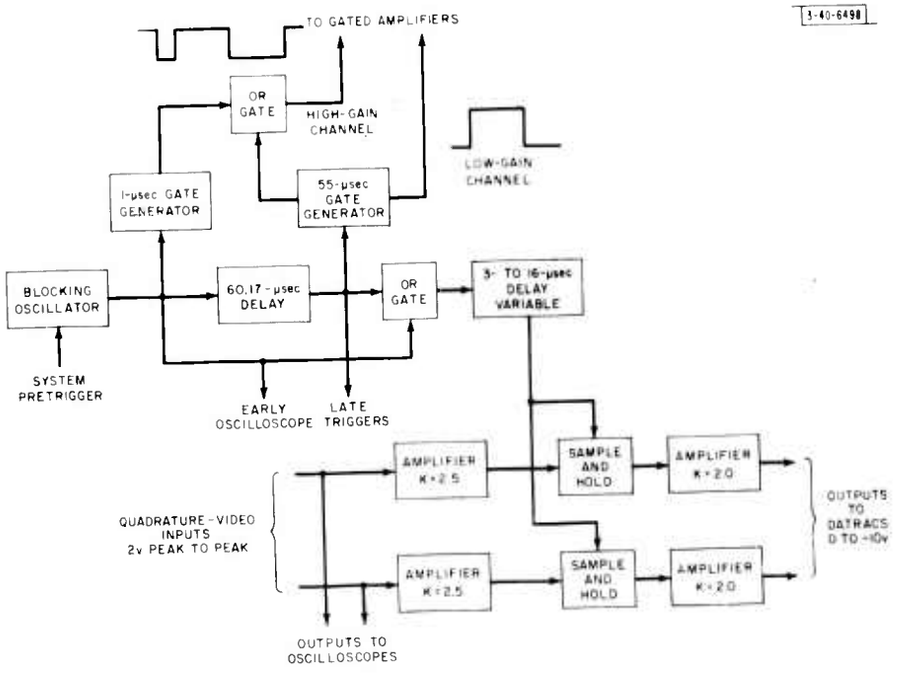

Fig. 62. Multiplex-timing and sample-and-hold chassis.

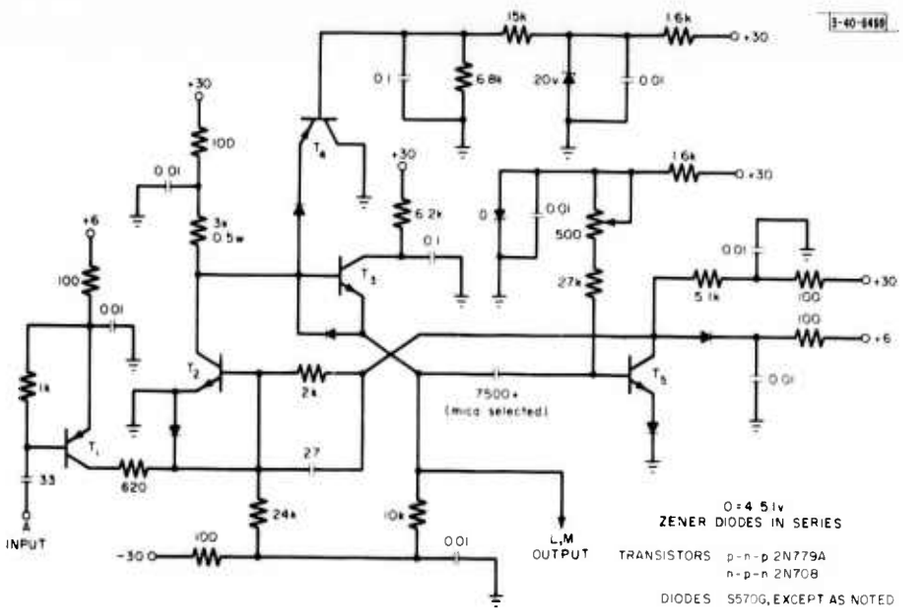

Fig. 63. 60.17-μsec delay schematic.

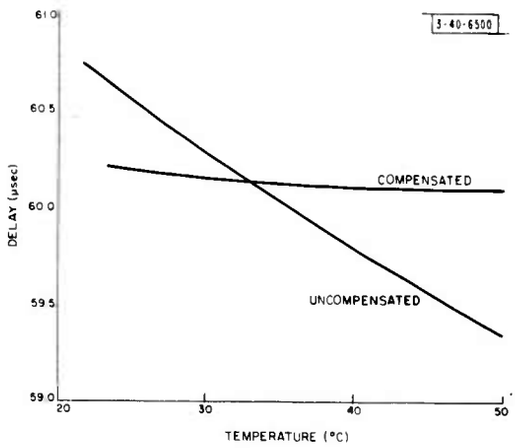

Fig. 64. 60.17-μsec delay vs temperature.

by the fact that the temperature coefficient of a Zener diode depends on its breakdown voltage; below 6 volts the coefficient is negative, above 6 volts it is positive. It is possible, then, to make up a Zener diode of 20 volts, which has a temperature coefficient anywhere between ±0.1 percent/°C, simply by choosing the voltages of the individual diodes, which are connected in series, to obtain the 20 volts. If the Zener diode D (shown in Fig. 63), is given an appropriate negative temperature coefficient, the delay instabilities due to the temperature-dependent terms mentioned previously, can be minimized by a factor of ten. If the clamping diode for the collector of T_2 is connected to +6 volts, instead of the emitter of T_4, and if the timing resistance (27 kohm plus a 500-ohm potentiometer) is connected to +20 volts, and is not connected as shown, the delay vs temperature characteristic of Fig. 64 is obtained (marked uncompensated). If, however, the circuit is connected as shown in the schematic, the curve marked compensated is obtained. It can be seen that the delay changes by 50 nsec with a temperature change from 30° to 40°C. Jitter is less than 10 nsec.

A pair of complementary gates is generated by a 55-μsec multivibrator, to turn on and off, at appropriate times, the gated IF amplifiers in the high- and low-gain channels of the multiplex chassis. In addition, the high-gain channel is turned off for one microsecond immediately after the range-gate pretrigger in order to establish a noise-free reference for the high-gain channel camera display, which will aid in the data reduction of the film.

A pair of pulses is generated to trigger the oscilloscopes used for the camera displays. The first pulse, at the time of the system pretrigger, triggers the oscilloscope which displays the high-gain channel video, while the second pulse, 60.17 μsec later, triggers the oscilloscope which displays the low-gain channel video. It should be noted that the output of each quadrature-video phase detector is connected to the sample-and-hold chassis through a 50-ohm cable. The high-impedance inputs of the boxcar input amplifiers (4 kohm and 5 pf) are tapped off each cable. Each video signal is then connected by another length of 50-ohm cable to the two inputs of the first camera display oscilloscope. These inputs are connected with another pair of coaxial cables to the second oscilloscope where each line is terminated in 50 ohms. This termination is important because it is the termination for the output of the phase detector.

The remaining timing circuitry is straightforward. All rise and fall times are kept to less than 20 nsec, so that any timing instability will be less than the 50-nsec aperture of the boxcar.

D. Test Pulse Generator

The two multivibrator delays in the sample-and-hold chassis must be set to an accuracy of better than 50 nsec. The 3- to 16-μsec variable delay must equal the amount of time by which the system pretrigger precedes the target leading edge; the 60.17-μsec delay must equal the multiplexing delay. The test pulse generator provides a means for adjusting these two delays.

A block diagram of the generator is shown in Fig. 65. A 60-Mcps, 0.07-μsec pulse is generated within 3 to 16 μsec after the system pretrigger (an internally generated 1-kcps trigger can also be switch selected). The exact amount by which this test pulse is delayed is determined by a multivibrator delay and can be set up by using an oscilloscope to make a simultaneous comparison with a synchronous delay known to be correct. The test pulse is applied to the IF input of the multiplex chassis. The multiplexed and phase-detected output of this chassis is sent to the boxcar inputs. By observing a boxcar output, the two delays in the sample-and-hold chassis can be set to the desired value by first adjusting the 3- to 16-μsec variable delay until the high-gain quadrature-video output pulse is observed in the boxcar output. The low-gain (delayed)

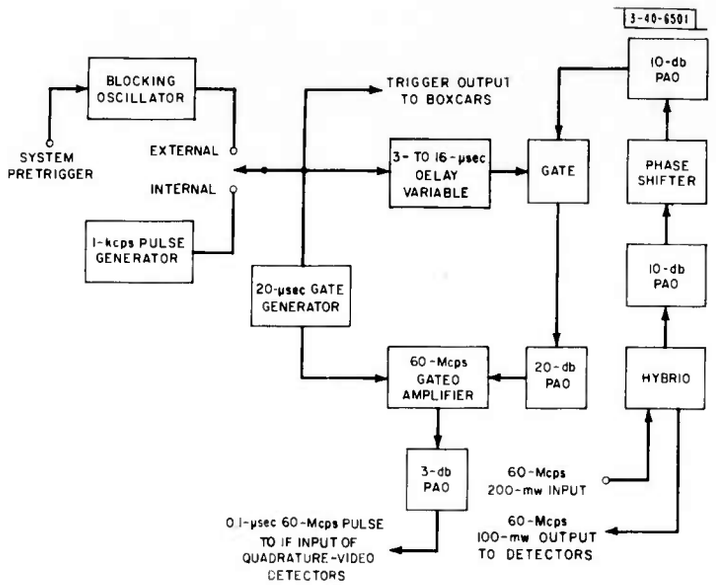

Fig. 65. Test-pulse generatar.

Fig. 66. Display and recarding equipment.

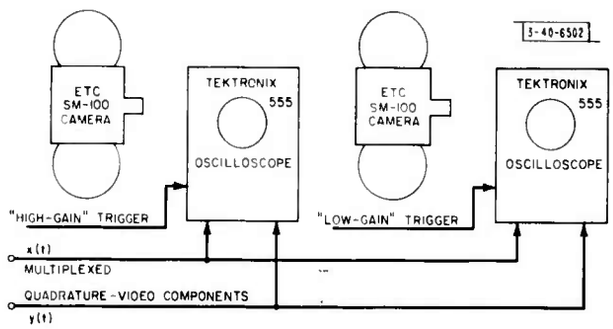

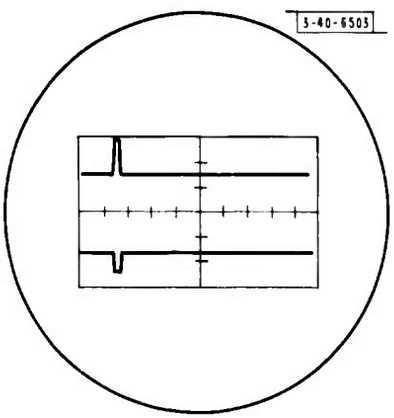

Fig. 67. Single-frame ascilloscope display (1 valt/cm vertical, 2 μsec/cm harizontal).

video output will then be observed in the boxcar output when the 60.17-μsec delay is correctly adjusted. Since the test pulse is slightly wider than the aperture of the boxcars, the delay adjustments will have to be set to the center of the range which produces the appropriate boxcar outputs. The accuracy of calibration, however, should be better than 35 nsec.

V. DISPLAY AND RECORDING EQUIPMENT

The recording and display equipment was assembled by Group 47 for their coherent radar experiments with the UHF radar at Wallops Island. Parallel photographic equipment, not described here, is used by the Re-entry Physics Program, as is the DATRAC digital recording of the sampled data described in the preceding section.

The equipment consists of two Tektronix dual-beam oscilloscopes viewed by two modified Electron Tube Corporation (ETC) Model SM-100 strip-film cameras, as illustrated in Fig. 66. Since the high- and low-gain signals are separated in their time of occurrence by the IF multiplexing equipment, they are individually displayed on the two oscilloscopes by triggering the oscilloscopes with the high-gain and low-gain triggers, respectively, provided in the timing generation equipment.

Figure 67 illustrates the oscilloscope display of the quadrature-video components for a single range sweep. In order to prevent overlap of the traces, the peak-to-peak amplitude is less than 3 cm on each trace. The gain of the high-gain channel must be adjusted so that the front-end receiver noise is barely measurable on the display, thus assuring a high sensitivity. The gain in the low-gain channel must be adjusted so that, at a signal level corresponding to the 3-cm peak-to-peak maximum deflection on the high-gain display, the deflection on the low-gain display is just barely measurable. These adjustments then assure the maximum possible dynamic range without loss of intermediate amplitude data.

The basic problem with this method of recording is the resolution afforded by the oscilloscopes, which are limited by their spot size of about 25 mils. In order to preserve as much resolution as possible, the full 10-cm horizontal display is employed using a sweep rate of about 2 μsec/cm which is required in order to display the maximum wake lengths expected.

The strip-film cameras operate with 1000-ft reels of 35-mm film and transport the film continuously at a rate of 16.5 ft/sec; therefore, about one minute of recording time is available. The direction of the film travel is transverse to the oscilloscope sweep. In order to prevent overlap of successive frames on the film when the radar is operated at its maximum repetition rate of 960 pps, the image size has been reduced to about half that normally afforded by the ETC cameras by modifying the lens assembly.

Some comparison has been made among various film types including Plus X, Royal X Pan, and Tri-X films. Our experience has shown that the Tri-X film yields the best results, and if this is borne out by further experiments, Tri-X film will be used.

VI. EPILOGUE

In most respects our estimates of the difficulties involved in the modification were reasonably accurate. Only in the case of the transmitter did we underestimate the difficulties. The modulator proved to be unreliable when the pulse repetition rate was increased from 320 to 960 pps. This problem was solved adequately without serious delay in our schedule. The synchronizer, which supplies timing not only to the UHF radar but also to the S-band radar and its

tracking circuitry, also required some unanticipated effort. This unit was completely replaced, resulting in a substantial improvement in timing stability, not only in the new 960-pps mode of operation but also in the old 320-pps mode.

As indicated in Sec. II, the transmission-line system required considerable correction. We considered that, after correction, the system had acceptable, if not desirable, VSWR characteristics. When the radar was placed in operation, we encountered a phenomenon which we should have anticipated, but did not. In flight tests conducted with balloons, we noticed an echo that was delayed behind the main target response by approximately 0.5 μsec. This delay corresponds to twice the time of transmission through the waveguide connecting the transmitter to the antenna feed. It was therefore probably due to a reflection from the feed being again reflected at the final amplifier.

The level of this delayed signal was reduced to a value 20 db less than the primary transmission by selecting an operating frequency region where the VSWR was low. The level will be reduced further by insertion of an isolator in the transmission-line system between the final amplifier and the feed. Our experience with the transmitter indicates that it constitutes a problem area for systems having wide bandwidth transmissions and long transmission-line paths.

The installation of equipment was completed in December 1962, approximately seven months after the initiation of the program. To date, the new equipment has performed satisfactorily during three Trailblazer re-entries. Although the recorded data have still to be reduced and evaluated, early indications are that much useful information will be obtained. Of particular interest is the Trailblazer IIc exercise in which data were obtained on both the last-stage rocket motor and the payload for more than one minute, which encompassed exoatmospheric and re-entry portions of the flight.

To assume adequate signal-to-noise ratio, a 1-μsec pulse width was used in this experiment.

UNCLASSIFIED